

Rungs 1 to 4 of DFT Jacob's ladder: Extensive test on the lattice constant, bulk modulus, and cohesive energy of solids

Fabien Tran, Julia Stelzl, and Peter Blaha

Citation: *The Journal of Chemical Physics* **144**, 204120 (2016); doi: 10.1063/1.4948636

View online: <http://dx.doi.org/10.1063/1.4948636>

View Table of Contents: <http://scitation.aip.org/content/aip/journal/jcp/144/20?ver=pdfcov>

Published by the **AIP Publishing**

Articles you may be interested in

[Exact two-component relativistic energy band theory and application](#)

J. Chem. Phys. **144**, 044105 (2016); 10.1063/1.4940140

[A DFT study on structural, vibrational properties, and quasiparticle band structure of solid nitromethane](#)

J. Chem. Phys. **138**, 184705 (2013); 10.1063/1.4803479

[Periodic local Møller–Plesset second order perturbation theory method applied to molecular crystals: Study of solid NH₃ and CO₂ using extended basis sets](#)

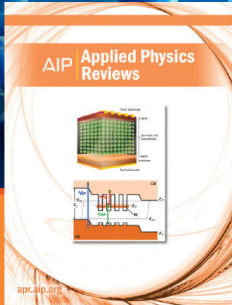
J. Chem. Phys. **132**, 134706 (2010); 10.1063/1.3372800

[Range separated hybrid density functional with long-range Hartree-Fock exchange applied to solids](#)

J. Chem. Phys. **127**, 054101 (2007); 10.1063/1.2759209

[Influence of electronic correlations on the ground-state properties of cerium dioxide](#)

J. Chem. Phys. **124**, 234711 (2006); 10.1063/1.2206187



NEW Special Topic Sections

NOW ONLINE
Lithium Niobate Properties and Applications:
Reviews of Emerging Trends

AIP | Applied Physics
Reviews

Rungs 1 to 4 of DFT Jacob's ladder: Extensive test on the lattice constant, bulk modulus, and cohesive energy of solids

Fabien Tran, Julia Stelzl, and Peter Blaha

Institute of Materials Chemistry, Vienna University of Technology, Getreidemarkt 9/165-TC, A-1060 Vienna, Austria

(Received 4 March 2016; accepted 22 April 2016; published online 27 May 2016)

A large panel of old and recently proposed exchange-correlation functionals belonging to rungs 1 to 4 of Jacob's ladder of density functional theory are tested (with and without a dispersion correction term) for the calculation of the lattice constant, bulk modulus, and cohesive energy of solids. Particular attention will be paid to the functionals MGGA_MS2 [J. Sun *et al.*, J. Chem. Phys. **138**, 044113 (2013)], mBEEF [J. Wellendorff *et al.*, J. Chem. Phys. **140**, 144107 (2014)], and SCAN [J. Sun *et al.*, Phys. Rev. Lett. **115**, 036402 (2015)] which are meta-generalized gradient approximations (meta-GGA) and are developed with the goal to be universally good. Another goal is also to determine for which semilocal functionals and groups of solids it is beneficial (or not necessary) to use the Hartree-Fock exchange or a dispersion correction term. It is concluded that for strongly bound solids, functionals of the GGA, i.e., rung 2 of Jacob's ladder, are as accurate as the more sophisticated functionals of the higher rungs, while it is necessary to use dispersion corrected functionals in order to expect at least meaningful results for weakly bound solids. If results for finite systems are also considered, then the meta-GGA functionals are overall clearly superior to the GGA functionals. *Published by AIP Publishing.* [<http://dx.doi.org/10.1063/1.4948636>]

I. INTRODUCTION

Starting in the mid 1980s,^{1,2} there has been a constantly growing interest in the development of exchange-correlation (xc) functionals $E_{xc} = E_x + E_c$ in the Kohn-Sham (KS) density functional theory (DFT),^{3,4} and the number of functionals that have been proposed so far is rather huge (see, e.g., Refs. 5–8 for recent reviews). This is understandable since KS-DFT is the most used method for the theoretical modeling of solids, surfaces, and molecules at the quantum level, and the accuracy of a KS-DFT calculation depends to a large extent on the chosen approximation for E_{xc} . Over the years, the degree of sophistication of the functionals (and their accuracy) has increased and most of the functionals belong to one of the rungs of Jacob's ladder.^{9,10} On the first three rungs, there are the so-called semilocal (SL) approximations which consist of a single integral for E_{xc} ,

$$E_{xc}^{SL} = \int \epsilon_{xc}(\mathbf{r}) d^3r, \quad (1)$$

and where ϵ_{xc} , the exchange-correlation energy density per volume, is a function of (a) the electron density $\rho = \sum_{i=1}^N |\psi_i|^2$ in the local density approximation (LDA, first rung), (b) ρ and its first derivative $\nabla\rho$ in the generalized gradient approximation (GGA, second rung), and (c) ρ , $\nabla\rho$, and the kinetic-energy (KE) density $t = (1/2) \sum_{i=1}^N \nabla\psi_i^* \cdot \nabla\psi_i$ and/or $\nabla^2\rho$ in the meta-GGA approximation (MGGA, third rung). On the fourth rung there are the functionals which make use of the [full or short-range (SR)] Hartree-Fock (HF) exchange, like the hybrid functionals,¹¹

$$E_{xc}^{hybrid} = E_{xc}^{SL} + \alpha_x (E_x^{(SR)\text{-HF}} - E_x^{(SR)\text{-SL}}), \quad (2)$$

where α_x ($\in [0, 1]$) is the fraction of HF exchange energy $E_x^{(SR)\text{-HF}}$ which is a double integral,

$$E_x^{(SR)\text{-HF}} = -\frac{1}{2} \sum_{i=1}^N \sum_{j=1}^N \delta_{\sigma_i\sigma_j} \int \int \psi_i^*(\mathbf{r}) \psi_j(\mathbf{r}) \times v(|\mathbf{r} - \mathbf{r}'|) \psi_j^*(\mathbf{r}') \psi_i(\mathbf{r}') d^3r d^3r', \quad (3)$$

where the indices i and j run over the occupied orbitals and v is the Coulomb potential $1/|\mathbf{r} - \mathbf{r}'|$ or only the SR part of it^{12,13} (i.e., a screened potential). On the fifth rung of Jacob's ladder, there are the functionals which utilize all (occupied and unoccupied) orbitals, like the random phase approximation (RPA, see, e.g., Refs. 14 and 15).

The functionals of the first four rungs have been extremely successful in describing the properties of all kinds of electronic systems, ranging from atoms to solids.^{5–7} However, a well-known problem common to *all* these functionals is that the long-range London dispersion interactions (always attractive and resulting from the interaction between non-permanent multipoles) are formally not included. In the case of two nonoverlapping spherical atoms, these functionals give an interaction energy of strictly zero, which is not the case in reality because of the attractive London dispersion interactions. As a consequence, the results obtained with the semilocal and hybrid functionals on systems where the London dispersion interactions play a major role can be qualitatively wrong.¹⁶ Nevertheless, as underlined in Ref. 17, at equilibrium geometry the overlap between two interacting entities is not zero, such that a semilocal or hybrid xc-functional can eventually lead to a non-zero contribution to the interaction energy and

therefore, possibly useful results (see, e.g., Ref. 18). In order to improve the reliability of KS-DFT calculations for such systems, functionals including the dispersion interactions in their construction were proposed. A simple and widely used method consists of adding to the semilocal or hybrid functional an atom-pairwise (PW) term of the form

$$E_{c,disp}^{PW} = - \sum_{A < B} \sum_{n=6,8,10,\dots} f_n^{\text{damp}}(R_{AB}) \frac{C_n^{AB}}{R_{AB}^n}, \quad (4)$$

where C_n^{AB} are the dispersion coefficients for the atom pair A and B separated by the distance R_{AB} and f_n^{damp} is a damping function preventing Eq. (4) from becoming too large for small R_{AB} . The coefficients C_n^{AB} can be either precomputed (see, e.g., Refs. 19–24) or calculated using properties of the system like the atomic positions or the electron density (see, e.g., Refs. 25–27). The other group of well-known methods accounting explicitly of dispersion interactions consists of adding to $E_{xc}^{\text{SL/hybrid}}$ a nonlocal (NL, in the sense of being a double integral) term of the form²⁸

$$E_{c,disp}^{\text{NL}} = \frac{1}{2} \iint \rho(\mathbf{r}) \Phi(\mathbf{r}, \mathbf{r}') \rho(\mathbf{r}') d^3r d^3r', \quad (5)$$

where the kernel Φ depends on ρ and $\nabla\rho$ at \mathbf{r} and \mathbf{r}' as well as on $|\mathbf{r} - \mathbf{r}'|$. Several functionals of the form of Eq. (5) are available in the literature^{28–33} and good results can be obtained if the proper combination $E_{xc}^{\text{SL/hybrid}} + E_{c,disp}^{\text{NL}}$ is used (see, e.g., Refs. 29, 31, and 34). Overall, the KS-DFT+dispersion methods produce results which are more reliable when applied to systems where the dispersion plays a major role, and therefore, the very cheap atom-pairwise and not-too-expensive nonlocal methods are nowadays routinely applied (see Refs. 16, 35, and 36 for recent reviews).

At this point, we should certainly also mention that truly *ab initio* (beyond DFT) methods have been used for the calculation of geometrical and energetic properties of solids (the focus of the present work). This includes RPA, which has been shown during these last few years to be quite reliable in many situations (see, e.g., Refs. 15 and 37–39 for extensive tests), the quantum Monte Carlo methods as exemplified in Ref. 40 for the calculation of the lattice and bulk modulus of a set of solids, and the post-HF methods which, as expected, should converge to the exact results.⁴¹

Another well-known problem in KS-DFT, which we will not address in this work, is the inadequacy of the semilocal functionals (or more precisely of the potential $v_{xc} = \delta E_{xc} / \delta \rho$) for the calculation of band gaps, while the hybrid functionals work reasonably well in this respect, thanks to the nonlocal HF exchange (see, e.g., Refs. 42–44).

In the present work, a large number of functionals of rungs 1 to 4 of Jacob's ladder, with or without a dispersion term, are tested on solids for the calculation of lattice constant, bulk modulus, and cohesive energy. A particular focus will be on the MGGA functionals recently proposed by Perdew and co-workers, namely, MGGA_MS (MGGA made simple),^{18,45,46} MVS (made very simple),⁴⁷ and SCAN (strongly constrained and appropriately normed semilocal density functional),⁴⁸ and by Wellendorff *et al.*,⁴⁹ mBEEF (model Bayesian error estimation functional), which should in principle be accurate semilocal functionals for both finite and

infinite systems, and to bind systems bound by weak interactions. Two testing sets of solids will be considered. The first one consists of cubic elemental solids and binary compounds bound by relatively strong interactions, while the second set is composed of systems bound mainly by weak interactions (e.g., dispersion). This extensive study of functionals performance on solids complements previous works, which include Refs. 50–60 for semilocal functionals, Refs. 42–44 and 61–64 for tests including hybrid functionals, Refs. 15, 37, and 38 for RPA, and Refs. 49 and 65–70 for a focus on functionals including dispersion via an atom-pairwise term or a nonlocal term.

The paper is organized as follows. The computational details are given in Sec. II. In Sec. III, the tested functionals are presented and some of their features are discussed. The results are presented and discussed in Sec. IV, while Sec. V gives a brief literature overview of the accuracy of functionals for the energetics of molecules. Finally, Sec. VI gives a summary of this work.

II. COMPUTATIONAL DETAILS

All calculations were done with the WIEN2k code,⁷¹ which uses the full-potential (linearized) augmented plane-wave plus local orbitals method⁷² to solve the KS equations. The parameters of the calculations like the number of \mathbf{k} -points for the integration of the Brillouin zone or size of the basis set were chosen to be large enough such that the results are well converged.

In order to make the testing of the numerous functionals tractable (especially for the hybrids which use the expensive HF exchange), the results on the strongly bound solids (listed in Table I) were obtained non-self-consistently by using the PBE⁷³ orbitals and densities. According to tests, the error in the lattice constant induced by this non-self-consistent procedure should be in most cases below 0.005 Å. The worst cases are the very heavy alkali and alkali-earth metals (Cs in particular) for which the error can be of the order of ~ 0.02 Å. Errors in the range 0.005–0.015 Å can eventually be obtained in the

TABLE I. The test set of 44 strongly and 5 weakly bound solids considered in this work. The space group is indicated in parentheses. With the exception of hexagonal graphite and h-BN, all solids are cubic.

Strongly bound solids	
C ($Fd\bar{3}m$), Si ($Fd\bar{3}m$), Ge ($Fd\bar{3}m$), Sn ($Fd\bar{3}m$), SiC ($F\bar{4}3m$),	
BN ($F\bar{4}3m$), BP ($F\bar{4}3m$), AlN ($F\bar{4}3m$), AlP ($F\bar{4}3m$), AlAs ($F\bar{4}3m$),	
GaN ($F\bar{4}3m$), GaP ($F\bar{4}3m$), GaAs ($F\bar{4}3m$), InP ($F\bar{4}3m$),	
InAs ($F\bar{4}3m$), InSb ($F\bar{4}3m$), LiH ($Fm\bar{3}m$), LiF ($Fm\bar{3}m$),	
LiCl ($Fm\bar{3}m$), NaF ($Fm\bar{3}m$), NaCl ($Fm\bar{3}m$), MgO ($Fm\bar{3}m$),	
Li ($Im\bar{3}m$), Na ($Im\bar{3}m$), Al ($Fm\bar{3}m$), K ($Im\bar{3}m$), Ca ($Fm\bar{3}m$),	
Rb ($Im\bar{3}m$), Sr ($Fm\bar{3}m$), Cs ($Im\bar{3}m$), Ba ($Im\bar{3}m$), V ($Im\bar{3}m$),	
Ni ($Fm\bar{3}m$), Cu ($Fm\bar{3}m$), Nb ($Im\bar{3}m$), Mo ($Im\bar{3}m$), Rh ($Fm\bar{3}m$),	
Pd ($Fm\bar{3}m$), Ag ($Fm\bar{3}m$), Ta ($Im\bar{3}m$), W ($Im\bar{3}m$), Ir ($Fm\bar{3}m$),	
Pt ($Fm\bar{3}m$), Au ($Fm\bar{3}m$)	
Weakly bound solids	
Ne ($Fm\bar{3}m$), Ar ($Fm\bar{3}m$), Kr ($Fm\bar{3}m$), graphite ($P6_3/mmc$),	
h-BN ($P6_3/mmc$)	

case of metals with hybrid functionals (a comparison can be done with our self-consistent hybrid calculations reported in Refs. 74 and 75). For the cohesive energy, the effect should not exceed 0.05 eV/atom except in the eventual cases where self-consistency would lead to an atomic electronic configuration for the isolated atom that is different from the one obtained with PBE. For the very weakly bound rare-gas solids, Ne, Ar, and Kr, and layered solids, graphite and h-BN, we observed that self-consistency may have a larger impact on the results (up to a few 0.1 Å in the case of very shallow total-energy curves), therefore the calculations were done self-consistently for LDA/GGA, but not for the MGGA functionals (not implemented self-consistently in WIEN2k) as well as the very expensive hybrid functionals.

The results of our calculations for the strongly bound solids were compared with experimental results that were corrected for thermal and zero-point vibrational effects (see Refs. 43 and 76). For the weakly bound systems, the results were compared with accurate *ab initio* results: coupled cluster with singlet, doublet, and perturbative triplet [CCSD(T)] for the rare gases⁷⁷ and RPA for the layered solids.^{78,79}

At this point, we should remind that in general, the observed trends in the relative performance of the functionals may depend on the test set and more particularly on the diversity of solids. Since our test set contains elements from all parts of the periodic table except lanthanides and actinides, our results should give a rather fair and unbiased overview of the accuracy of the functionals.

Finally, we mention that we did not include ferromagnetic bcc Fe in our test set of solids, since the total-energy curves exhibit a discontinuity at the lattice constant of ~ 2.94 Å (same value as found in Ref. 38), which is due to a change in orbitals occupation with PBE. This discontinuity is very large when the HF exchange is used, making an unambiguous determination of the equilibrium volume not possible with some of the hybrid functionals.

III. THE FUNCTIONALS

The exchange-correlation functionals that were tested for the present work are listed in Table II. They are grouped into families, namely, LDA, GGA, and MGGA, and their extensions that use the HF exchange, Eq. (2), [hybrid-...], a dispersion correction of the atom-pairwise type as given by Eq. (4) [...+D], or both. Among the GGA functionals, BLYP^{93,94} and PBE⁷³ have been the most used in chemistry and physics, respectively. PBE leads to reasonable results for solids (lattice constant and cohesive energy), while BLYP is much more appropriate for the atomization energy of molecules. More recent GGA functionals are AM05,⁸⁴ WC,⁸¹ SOGGA,⁸² and PBEsol,⁸³ which are more accurate for the lattice constant of solids (see, e.g., Ref. 54), but severely overbind molecules.⁸⁹ Other recent GGA functionals that were also tested are PBEint,⁸⁵ PBEfe,⁹⁰ and SG4.⁶⁰ In the group of MGGA functionals, there are the relatively old functionals PKZB⁹⁷ and TPSS,⁹⁶ as well as the very recent ones MGGA_MS2,^{18,46} mBEEF,⁴⁹ and SCAN,⁴⁸ which should be among the most accurate semilocal functionals for molecules and solids and also provide (possibly) useful results for weakly bound sys-

tems. The other recent MGGA MVS⁴⁷ is also among the tested functionals.

A semilocal functional can be defined by its xc-enhancement factor F_{xc} ,

$$F_{xc}(\mathbf{r}) = \frac{\epsilon_{xc}(\mathbf{r})}{\epsilon_x^{\text{LDA}}(\mathbf{r})} = \frac{\epsilon_x(\mathbf{r}) + \epsilon_c(\mathbf{r})}{\epsilon_x^{\text{LDA}}(\mathbf{r})} = F_x(\mathbf{r}) + F_c(\mathbf{r}), \quad (6)$$

where $\epsilon_x^{\text{LDA}} = -(3/4)(3/\pi)^{1/3}\rho^{4/3}$ is the exact exchange-energy density for constant electron densities.^{4,110,111} For convenience, F_{xc} is usually expressed as a function of the variables $r_s = (3/(4\pi\rho))^{1/3}$ (the radius of the sphere which contains one electron), $s = |\nabla\rho| / (2(3\pi^2)^{1/3}\rho^{4/3})$ (the reduced density gradient), and $\alpha = (t - t^W)/t^{\text{TF}}$ where $t^W = |\nabla\rho|^2 / (8\rho)$ is the von Weizsäcker¹¹² KE density (exact for systems with only one occupied orbital) and $t^{\text{TF}} = (3/10)(3\pi^2)^{2/3}\rho^{5/3}$ is the Thomas-Fermi KE density^{113,114} (exact for constant electron densities). Note that the exchange part F_x does not depend on r_s , but only on s (and α for MGGAs).

Figures 1 and 2 show the enhancement factor of most GGA and MGGA functionals tested in this work. Now, we summarize the trends in the performances of GGA functionals and how they are related to the shape of F_{xc} (mainly determined by the dominating exchange part F_x , see upper panel of Fig. 1). LDA, which has the *weakest* enhancement factor, underestimates the equilibrium lattice constant a_0 of solids. Since large unit cells contain more density gradient (i.e., larger s) than small unit cells, then a stronger F_{xc} (any GGA, see Fig. 1) will lower the total energy more for large unit cells than for smaller ones (a stronger F_{xc} makes the total energy more negative), and therefore reduce the underestimation of a_0 obtained with LDA. A good balance is obtained with *weak* GGAs like AM05 or PBEsol (see Fig. 1), which are among the most accurate for lattice constants. Concerning the cohesive energy E_{coh} of solids, LDA overestimates the values. Since an isolated atom contains much more density gradient than the solid, then a GGA (with respect to LDA) lowers the total energy of the atom by a larger amount than for the solid, thus reducing the overestimation of E_{coh} . In this respect, functionals with a *medium* F_{xc} like PBE do a pretty good job. GGAs with a *strong* F_{xc} like B88 or RPBE overcorrect LDA and lead to overestimation and underestimation of a_0 and E_{coh} , respectively. LDA overestimates the atomization energies of molecules as well, and, using the same argument as for E_{coh} , a GGA lowers (with respect to LDA) the total energy more for the atoms than for the molecule. However, in this case, functionals with a *strong* enhancement factor (e.g., B88) are the best performing GGAs, while weaker GGAs reduce only partially the LDA overestimation. One may ask the following question: Why is it necessary to use a F_{xc} that is stronger for the atomization energy of molecules than for the cohesive energy of solids? The reason is that the degrees of ρ -inhomogeneity in the solid and atom (both used to calculate E_{coh}) are very different, such that the appropriate difference (between the solid and atom) in the lowering of the total energy (with respect to LDA) is already achieved with a weak F_{xc} . Since the atomization energy of molecules requires calculations on the atoms and molecule, which have more similar inhomogeneities (slightly larger in atoms than in molecule), then a stronger F_{xc} is required to

TABLE II. The ME, MAE, MRE, MARE, and MAXRE on the testing set of 44 strongly bound solids for the lattice constant a_0 , bulk modulus B_0 , and cohesive energy E_{coh} . The units of the ME and MAE are Å, GPa, and eV/atom for a_0 , B_0 , and E_{coh} , respectively, and % for the MRE, MARE, and MAXRE. The solid for which the MAXRE occurs is indicated in parentheses. All results were obtained non-self-consistently using PBE orbitals/density. Within each group, the functionals are ordered by increasing value of the MARE of a_0 . For hybrid functionals, the fraction α_x of HF exchange is indicated in parentheses.

Functional	a_0					B_0					E_{coh}				
	ME	MAE	MRE	MARE	MAXRE	ME	MAE	MRE	MARE	MAXRE	ME	MAE	MRE	MARE	MAXRE
LDA															
LDA ⁸⁰	-0.071	0.071	-1.5	1.5	-4.9 (Ba)	10.1	11.5	8.1	9.4	32.8 (Ni)	0.77	0.77	17.2	17.2	38.7 (Ni)
GGA															
SG4 ⁶⁰	0.005	0.026	0.0	0.6	-1.9 (V)	1.7	7.9	-2.2	7.8	-25.9 (Rb)	0.19	0.28	3.5	7.0	19.5 (Ni)
WC ⁸¹	0.002	0.029	0.0	0.6	-2.5 (Ba)	-0.2	7.6	-2.6	7.4	-23.8 (Rb)	0.22	0.26	4.2	6.2	20.1 (Ni)
SOGGA ⁸²	-0.012	0.027	-0.3	0.6	-2.3 (Ba)	4.1	8.9	0.6	7.4	23.6 (Ni)	0.39	0.41	8.8	9.2	26.8 (Ni)
PBEsol ⁸³	-0.005	0.030	-0.1	0.6	-2.3 (Sr)	0.7	7.8	-1.4	7.0	19.5 (Ni)	0.29	0.31	6.1	6.9	22.8 (Ni)
AM05 ⁸⁴	0.014	0.037	0.2	0.8	2.1 (NaF)	-0.3	8.8	-4.0	9.2	-25.9 (Rb)	0.30	0.45	7.6	12.6	90.4 (LiH)
PBEint ⁸⁵	0.026	0.039	0.5	0.8	2.5 (NaF)	-3.0	8.4	-5.3	8.7	-25.5 (Rb)	0.10	0.20	1.5	4.7	16.4 (Ni)
PBEalpha ⁸⁶	0.021	0.042	0.4	0.9	2.0 (Sn)	-6.0	8.4	-5.0	7.6	-21.2 (Ge)	0.10	0.18	1.8	4.1	14.5 (Ni)
RGE2 ⁸⁷	0.043	0.051	0.8	1.0	3.6 (Cs)	-4.3	9.0	-7.3	10.2	-31.5 (Rb)	0.00	0.20	-1.2	5.0	-14.9 (Au)
PW91 ⁸⁸	0.053	0.059	1.1	1.2	2.6 (Sn)	-11.0	12.1	-9.8	10.9	-25.3 (Ge)	-0.12	0.18	-3.5	4.6	-20.1 (Au)
PBE ⁷³	0.056	0.061	1.1	1.2	2.8 (Sn)	-11.2	12.2	-9.8	11.0	-25.5 (Ge)	-0.13	0.19	-3.9	5.0	-21.0 (Au)
HTBS ⁸⁹	0.068	0.077	1.3	1.6	8.1 (Cs)	-4.0	9.9	-9.4	12.7	-47.7 (Rb)	-0.14	0.23	-4.5	6.2	-20.1 (Cs)
PBEfe ⁹⁰	0.002	0.082	0.1	1.7	-4.9 (Cs)	-10.0	12.6	-3.3	11.2	-27.1 (Ge)	0.15	0.22	3.4	5.0	13.5 (Sn)
revPBE ⁹¹	0.106	0.107	2.2	2.2	5.4 (Cs)	-17.1	17.5	-16.0	16.4	-34.3 (Rb)	-0.48	0.48	-12.6	12.6	-34.2 (Au)
RPBE ⁹²	0.119	0.119	2.4	2.4	6.1 (Cs)	-19.0	19.3	-17.2	17.5	-35.1 (Au)	-0.52	0.52	-13.2	13.2	-36.7 (Au)
BLYP ^{93,94}	0.118	0.120	2.5	2.5	5.2 (Sn)	-25.1	25.2	-19.9	20.3	-44.6 (Au)	-0.69	0.69	-20.3	20.3	-52.8 (Cs)
MGGA															
MGGA_MS2 ⁴⁶	0.016	0.029	0.2	0.6	4.6 (Cs)	4.1	7.6	0.2	6.8	-23.7 (Rb)	0.06	0.21	0.9	5.2	20.0 (Cu)
SCAN ⁴⁸	0.018	0.030	0.3	0.6	3.8 (Cs)	3.5	7.4	-0.4	6.5	-22.0 (Rb)	-0.02	0.19	-0.7	4.9	-16.6 (Cs)
revTPSS ⁹⁵	0.023	0.039	0.4	0.8	3.3 (Cs)	-0.1	9.6	-3.4	9.4	-25.8 (Rb)	0.05	0.22	1.2	5.1	17.7 (Cu)
MGGA_MS0 ⁴⁵	0.032	0.044	0.5	0.9	6.3 (Cs)	4.2	8.3	-0.9	7.3	-27.5 (Rb)	-0.02	0.22	-1.2	5.2	17.8 (Ir)
MVS ⁴⁷	-0.008	0.043	-0.3	0.9	5.3 (Cs)	12.3	13.3	8.2	12.7	56.9 (Al)	0.21	0.37	5.8	9.3	33.0 (Cu)
mBEEF ⁴⁹	0.033	0.050	0.5	1.0	6.6 (Cs)	1.4	7.9	-1.4	7.8	-27.6 (Ba)	-0.13	0.21	-3.0	4.6	-17.0 (Au)
MGGA_MS1 ⁴⁶	0.045	0.054	0.8	1.1	6.8 (Cs)	1.8	8.1	-3.1	8.0	-29.7 (Rb)	-0.10	0.24	-3.3	5.9	-15.5 (Cs)
TPSS ⁹⁶	0.045	0.054	0.9	1.1	4.1 (Cs)	-4.6	9.6	-6.7	10.3	-29.6 (Rb)	-0.09	0.20	-2.3	4.9	-15.3 (Au)
PKZB ⁹⁷	0.086	0.088	1.7	1.8	7.9 (Cs)	-8.1	11.0	-10.0	12.4	-35.9 (NaF)	-0.30	0.34	-7.2	8.1	-23.4 (Au)
hybrid-LDA															
LDA ^{80,98} (0.25)	-0.036	0.037	-0.8	0.9	-3.3 (V)	12.0	12.6	7.2	8.7	35.6 (V)	0.03	0.31	0.1	7.5	-21.1 (V)
YSLDA ^{80,98} (0.25)	-0.041	0.041	-0.9	0.9	-3.3 (V)	11.7	12.2	7.2	8.6	35.0 (V)	0.16	0.30	3.6	6.8	17.1 (Sn)
hybrid-GGA															
YSPBEsol ⁴³ (0.25)	0.002	0.021	0.0	0.5	-2.7 (V)	6.9	8.7	1.5	6.9	30.3 (V)	-0.17	0.27	-4.0	6.0	-26.1 (V)
PBEsol ^{83,98} (0.25)	-0.011	0.021	-0.3	0.5	-2.9 (V)	10.3	11.1	4.4	7.9	33.0 (V)	-0.13	0.28	-3.3	6.5	-27.2 (V)
PBE ^{99,100} (0.25)	0.032	0.038	0.6	0.8	3.7 (Cs)	1.7	7.5	-1.8	6.9	26.4 (V)	-0.45	0.46	-10.7	10.9	-35.9 (V)
B3PW91 ¹¹ (0.20)	0.047	0.050	0.9	1.0	4.0 (Cs)	-3.0	7.5	-5.8	8.3	-28.9 (Rb)	-0.55	0.55	-14.1	14.1	-33.9 (V)
YSPBE ^{74,101} (0.25)	0.054	0.056	1.0	1.1	4.3 (Cs)	-3.3	8.0	-5.9	8.6	-27.7 (Rb)	-0.55	0.55	-12.9	12.9	-36.4 (V)
B3LYP ¹⁰² (0.20)	0.082	0.084	1.7	1.7	4.4 (Cs)	-13.3	14.5	-12.2	13.1	-39.4 (Au)	-0.84	0.84	-22.9	22.9	-51.9 (Cs)
hybrid-MGGA															
MGGA_MS2h ⁴⁶ (0.09)	0.012	0.027	0.1	0.6	4.9 (Cs)	7.4	8.8	2.2	7.1	24.1 (V)	-0.07	0.21	-2.0	5.1	-16.3 (V)
revTPSSH ¹⁰³ (0.10)	0.018	0.033	0.3	0.7	3.9 (Cs)	3.8	8.8	-1.0	8.1	-26.5 (Rb)	-0.09	0.18	-2.0	4.1	-10.7 (Au)
TPSS ^{96,98} (0.25)	0.025	0.039	0.4	0.8	5.2 (Cs)	6.6	9.2	0.5	8.1	32.1 (V)	-0.41	0.42	-9.3	9.4	-33.4 (V)
TPSSH ¹⁰⁴ (0.10)	0.037	0.044	0.7	0.9	4.5 (Cs)	-0.1	7.7	-3.8	8.4	-29.5 (Rb)	-0.22	0.25	-5.2	5.7	-18.6 (Au)
MVSh ⁴⁷ (0.25)	-0.013	0.055	-0.4	1.2	5.9 (Cs)	19.5	20.3	11.8	16.2	52.0 (Al)	-0.19	0.39	-3.4	8.7	-38.4 (V)
GGA+D															
PBEsol-D3 ¹⁰⁵	-0.031	0.039	-0.7	0.9	-3.3 (Ba)	5.9	10.0	2.7	7.3	27.9 (Cu)	0.50	0.50	11.7	11.7	29.1 (Ni)
PBE-D3 ²⁷	0.022	0.042	0.4	0.9	2.2 (Sn)	-4.8	8.7	-5.0	8.3	-25.3 (Ge)	0.12	0.16	2.9	3.9	14.1 (Ni)
PBE-D3(BJ) ¹⁰⁶	-0.002	0.042	-0.1	0.9	-3.1 (Li)	-3.1	7.5	-2.1	7.4	-22.6 (Ge)	0.20	0.21	4.8	5.2	15.7 (Ni)
revPBE-D3(BJ) ¹⁰⁶	-0.011	0.043	-0.4	1.0	-4.8 (Li)	-0.4	8.5	-1.4	8.6	-23.2 (Ge)	0.18	0.21	4.2	5.2	18.7 (Cu)
revPBE-D3 ²⁷	0.042	0.060	0.7	1.2	4.7 (NaF)	-6.9	11.9	-7.4	13.4	-49.5 (NaF)	-0.02	0.18	-0.3	4.4	13.9 (Na)
PBEsol-D3(BJ) ¹⁰⁵	-0.060	0.061	-1.3	1.3	-5.1 (Ba)	8.6	11.2	6.2	8.7	31.3 (Cu)	0.62	0.62	14.9	14.9	31.5 (Ni)
RPBE-D3 ¹⁰⁷	0.063	0.070	1.2	1.4	5.8 (NaF)	-13.9	15.2	-10.6	14.1	-41.6 (Au)	-0.14	0.20	-2.9	5.0	14.0 (Na)

TABLE II. (Continued.)

Functional	a_0					B_0					E_{coh}				
	ME	MAE	MRE	MARE	MAXRE	ME	MAE	MRE	MARE	MAXRE	ME	MAE	MRE	MARE	MAXRE
BLYP-D3 ²⁷	0.043	0.070	0.7	1.4	-4.6 (Li)	-12.3	16.1	-10.5	15.6	-46.7 (Au)	-0.18	0.24	-6.6	7.7	-33.3 (Sr)
BLYP-D3(BJ) ¹⁰⁶	-0.034	0.074	-0.8	1.6	-7.9 (Li)	-5.7	10.8	-1.0	10.6	-35.4 (Ge)	0.11	0.21	0.8	6.1	-23.6 (Cs)
MGGA+D															
MGGA_MS2-D3 ⁴⁶	0.002	0.030	-0.1	0.6	4.5 (Cs)	7.5	9.9	2.7	8.1	30.4 (Cu)	0.17	0.25	3.7	5.8	25.8 (Cu)
MGGA_MS0-D3 ⁴⁶	0.019	0.040	0.2	0.8	6.2 (Cs)	7.6	10.5	1.5	8.9	-28.6 (Rb)	0.08	0.21	1.5	4.9	21.2 (Ir)
MGGA_MS1-D3 ⁴⁶	0.026	0.047	0.4	1.0	6.6 (Cs)	6.4	10.5	0.2	8.9	28.7 (Cu)	0.05	0.20	0.5	4.6	20.0 (Ir)
TPSS-D3 ²⁷	-0.004	0.045	-0.3	1.0	-3.1 (V)	5.9	14.0	0.9	11.2	37.5 (Cu)	0.27	0.30	7.5	8.1	26.8 (Cu)
TPSS-D3(BJ) ¹⁰⁶	-0.042	0.049	-1.0	1.1	-4.1 (Li)	8.7	12.9	5.1	10.3	39.9 (Cu)	0.42	0.42	11.0	11.1	31.1 (Cu)
hybrid-GGA+D															
PBE0-D3 ²⁷ (0.25)	-0.005	0.027	-0.3	0.6	-3.2 (V)	9.3	11.7	4.0	9.0	37.7 (V)	-0.16	0.23	-2.9	4.8	-25.9 (V)
YSPBE0-D3(BJ) ¹⁰⁸ (0.25)	-0.023	0.030	-0.6	0.7	-3.3 (V)	7.8	9.9	4.4	7.7	35.4 (V)	-0.10	0.22	-0.9	5.2	-22.8 (Ni)
PBE0-D3(BJ) ¹⁰⁶ (0.25)	-0.030	0.035	-0.7	0.8	-3.3 (V)	11.3	12.2	7.2	9.3	37.0 (V)	-0.07	0.24	-0.7	5.2	-22.4 (V)
YSPBE0-D3 ¹⁰⁷ (0.25)	0.035	0.042	0.6	0.8	4.1 (Cs)	0.8	7.4	-3.0	7.5	27.5 (V)	-0.41	0.41	-9.3	9.4	-31.9 (V)
B3LYP-D3 ²⁷ (0.20)	0.018	0.047	0.2	1.0	-3.3 (V)	-1.3	10.5	-3.1	11.3	-39.5 (Au)	-0.38	0.38	-10.2	10.4	-33.5 (Sr)
B3LYP-D3(BJ) ¹⁰⁶ (0.20)	-0.043	0.055	-1.0	1.2	-6.1 (Li)	4.0	8.7	4.9	8.7	36.5 (V)	-0.15	0.22	-4.6	6.4	-26.0 (Cs)
hybrid-MGGA+D															
MGGA_MS2h-D3 ⁴⁶ (0.09)	-0.002	0.030	-0.2	0.7	4.8 (Cs)	10.9	11.7	4.7	9.1	27.7 (V)	0.04	0.21	0.8	5.1	18.8 (Cu)
TPSSh-D3 ¹⁰⁵ (0.10)	-0.013	0.040	-0.5	0.9	-3.5 (V)	10.6	14.5	4.1	11.1	39.2 (V)	0.16	0.19	5.0	5.7	20.6 (Cu)
TPSS0-D3 ²⁷ (0.25)	-0.023	0.045	-0.7	1.1	-4.0 (V)	17.6	18.7	8.6	13.4	48.6 (V)	-0.03	0.20	0.9	5.1	-20.0 (V)
TPSSh-D3(BJ) ¹⁰⁹ (0.10)	-0.049	0.054	-1.2	1.2	-4.1 (LiH)	13.5	15.0	8.3	11.4	38.5 (V)	0.30	0.30	8.5	8.5	24.7 (Cu)
TPSS0-D3(BJ) ¹⁰⁶ (0.25)	-0.064	0.068	-1.5	1.6	-4.3 (V)	20.9	21.0	14.0	15.3	48.2 (V)	0.13	0.24	4.9	7.0	17.7 (Na)

achieve the desired difference (between the atoms and the molecule) in the lowering of the total energy (with respect to LDA).

The above trends hold for GGA functionals that are conventional in the sense that F_{xc} does not exhibit a strange behavior like oscillations or a suddenly large slope $\partial F_{\text{xc}}/\partial s$ in a small region of s . More unconventional forms for F_{xc} are usually obtained when F_{xc} contains empirical parameters that are determined by a fit of reference data. The problem of such functionals is a reduced degree of transferability and clear failures in particular cases. An example of such a functional is given by the GGA exchange HTBS⁸⁹ (shown in Fig. 1) that was an attempt to construct a functional which leads to good results for both the lattice constants of solids and atomization energies of molecules: $F_{\text{x}}^{\text{HTBS}} = F_{\text{x}}^{\text{WC}}$ for $s < 0.6$ (weak GGA for s values relevant for solids) and $F_{\text{x}}^{\text{HTBS}} = F_{\text{x}}^{\text{RPBE}}$ for $s > 2.6$ (strong GGA for s values relevant for finite systems), while a linear combination of WC and RPBE is used for $s \in [0.6, 2.6]$. The results were shown to be very good except for systems containing alkali metals whose lattice constants are largely overestimated,⁸⁹ which is due to the large values of s in the core-valence separation region of the alkali metals (see Ref. 115).

Concerning the correlation enhancement factor F_{c} (see lower panel of Fig. 1), we just note that for LYP it behaves differently from the others and that the LDA limit is not recovered, since LYP was designed to reproduce the correlation energy of the helium atom and not of a constant electron density.⁹⁴

In Fig. 2, the total enhancement factor F_{xc} of MGGA is plotted as a function of s for three values of α (on the left

panels) and as a function of α for three values of s (on the right panels). The three values of α correspond to regions dominated by a single orbital ($\alpha = 0$), of constant electron density ($\alpha = 1$), and of overlap of closed shells ($\alpha \gg 5$).¹⁸ A few comments can be made. As mentioned above, it can happen for parameterized functionals, like the Minnesota suite of functionals,¹¹⁶ to have an enhancement factor that shows features like bumps or oscillations that are unphysical and may lead to problems of transferability of the functional. Furthermore, such features lead to numerical noise.^{117,118} The mBEEF is such a highly parameterized functional, however, since its parameters were fitted with a regularization procedure,⁴⁹ the bump visible in Fig. 2 is moderate. A particularity of the SCAN and MVS enhancement factors is to be much more a decreasing function of s and α than the other functionals. Note also the very weak variation of F_{xc} with respect to α for the TPSS, revTPSS, and MGGA_MS2 functionals. For MGGA functionals, it is maybe more difficult than for GGAs to establish simple relations between the shape of F_{xc} and the trends in the results. Anyway, it is clear that the additional dependency on the KE density leads to more flexibility and therefore potentially more universal functionals. Finally, we mention Refs. 18 and 119, where it was argued that at small s , the enhancement factor should be a decreasing function of α in order to obtain a binding between weakly interacting systems, which is the case for MGGA_MS2, MVS, and SCAN as shown in Fig. 2.

The hybrid functionals can be split into two groups according to the type of HF exchange that is used: the ones that use the unscreened HF exchange and those using only the SR part that was obtained by means of the screened Yukawa potential

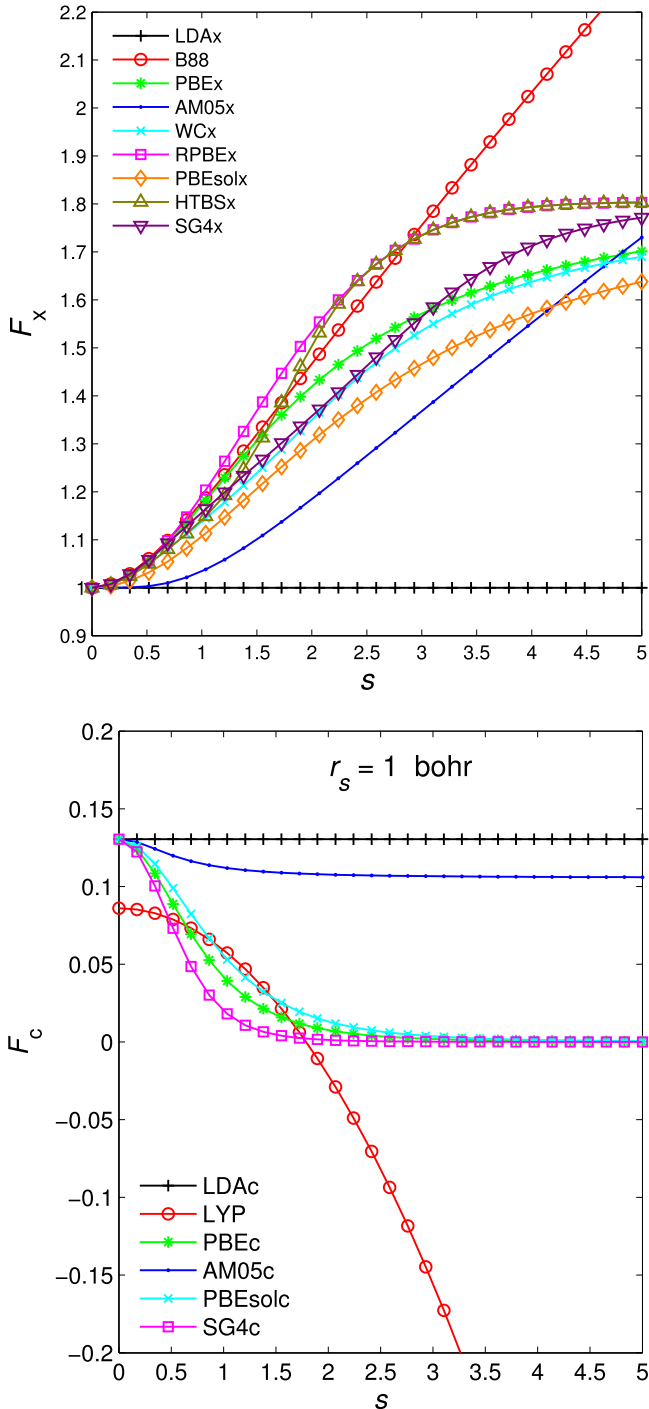


FIG. 1. GGA enhancement factors F_x (upper panel) and F_c (lower panel, for $r_s = 1$ bohr) plotted as a function of s .

(details of the implementation can be found in Ref. 74). From a technical point of view, the advantage of screened hybrid functionals over the unscreened ones is a faster convergence of the calculation of Eq. (3) with respect to the distance from the reference unit cell in real space integration or, equivalently, with respect to the number of \mathbf{k} -points in reciprocal space.¹³

The screened hybrid functionals in Table II are those whose name starts with YS (Yukawa screened), and among them, YSPBE0⁷⁴ is based on the popular functional of Heyd *et al.*^{13,101} HSE06 differs from it by the screening (Yukawa in YSPBE0 versus error function in HSE06) and the way

the screening is applied in the semilocal exchange (via the exchange hole¹³ or via the GGA enhancement factor¹²⁰). As noticed in Ref. 121, the error function- and Yukawa-screened potentials are very similar if the screening parameter in the Yukawa potential is 3/2 larger than in the error function. In Ref. 74, it was shown that HSE06 and YSPBE0 lead to basically the same band gaps, while non-negligible differences were observed for the lattice constants. A comparison between the YSPBE0 results obtained in the present work and the HSE06 results reported in Ref. 43 shows that the YSPBE0 lattice constants are in most cases slightly larger by 0.01-0.02 Å, while the atomization energies can differ by 0.05-0.2 eV/atom. Similarly, YSPBEsol0 uses the same underlying semilocal functional (PBEsol⁸³) and fraction of HF exchange (0.25) as HSEsol (Ref. 43). For all screened hybrid functionals tested in this work, a screening parameter $\lambda = 0.165$ bohr⁻¹ was used, which is 3/2 of the value used in HSE06 with the error function.¹⁰¹ The fraction α_x of HF exchange (indicated in Table II) varies between 0.09 (MGGA_MS2h) and 0.25 (e.g., PBE0).

Among the unscreened hybrid functionals in Table II, the two most well-known are B3LYP^{11,102} and PBE0.^{99,100} Note that in Refs. 75, 122, and 123, the use of screened and unscreened hybrid functionals for metals has been severely criticized, since qualitatively wrong results (e.g., incorrect prediction for the ground state or largely overestimated magnetic moment) were obtained for simple transition metals like Fe or Pd.

The two variants of atom-pairwise dispersion correction [Eq. (4)] that are considered were proposed by Grimme and co-workers.^{27,106} The two schemes, which use the position of atoms to calculate the dispersion coefficients C_n^{AB} , differ in the damping function f_n^{damp} . In the first scheme (DFT-D3, Ref. 27), the dispersion energy $E_{c,\text{disp}}^{\text{PW}}$ goes to zero when $R_{AB} \rightarrow 0$, while with the Becke-Johnson (BJ) damping function¹²⁴ that is used in DFT-D3(BJ),¹⁰⁶ $E_{c,\text{disp}}^{\text{PW}}$ goes to a nonzero value, which is theoretically correct.¹²⁵ All DFT-D3/D3(BJ) calculations were done with and without the three-body non-additive dispersion term,²⁷ which has little influence on the results for the strongly bound and rare-gas solids. For the layered compounds, however, the effect is larger since adding the three-body term increases the equilibrium lattice constant c_0 by ~ 0.1 Å and decreases the interlayer binding energy by ~ 10 meV/atom, which for the latter quantity leads to better agreement with the reference results in most cases. In the following, only the results including the three-body term will be shown, except for Table S22 of the supplementary material¹²⁶ which shows results for the layered compounds without three-body term. Note that in the case of YSPBE0-D3/D3(BJ), the parameters of the D3/D3(BJ) corrections are those that were proposed for the HSE06 functional. The DFT-D3/D3(BJ) dispersion energies were evaluated by using the package provided by Grimme¹⁰⁷ that supports periodic boundary conditions.^{108,127}

IV. RESULTS AND DISCUSSION

A. Strongly bound solids

Table II shows the mean error (ME), mean absolute error (MAE), mean relative error (MRE), mean absolute relative

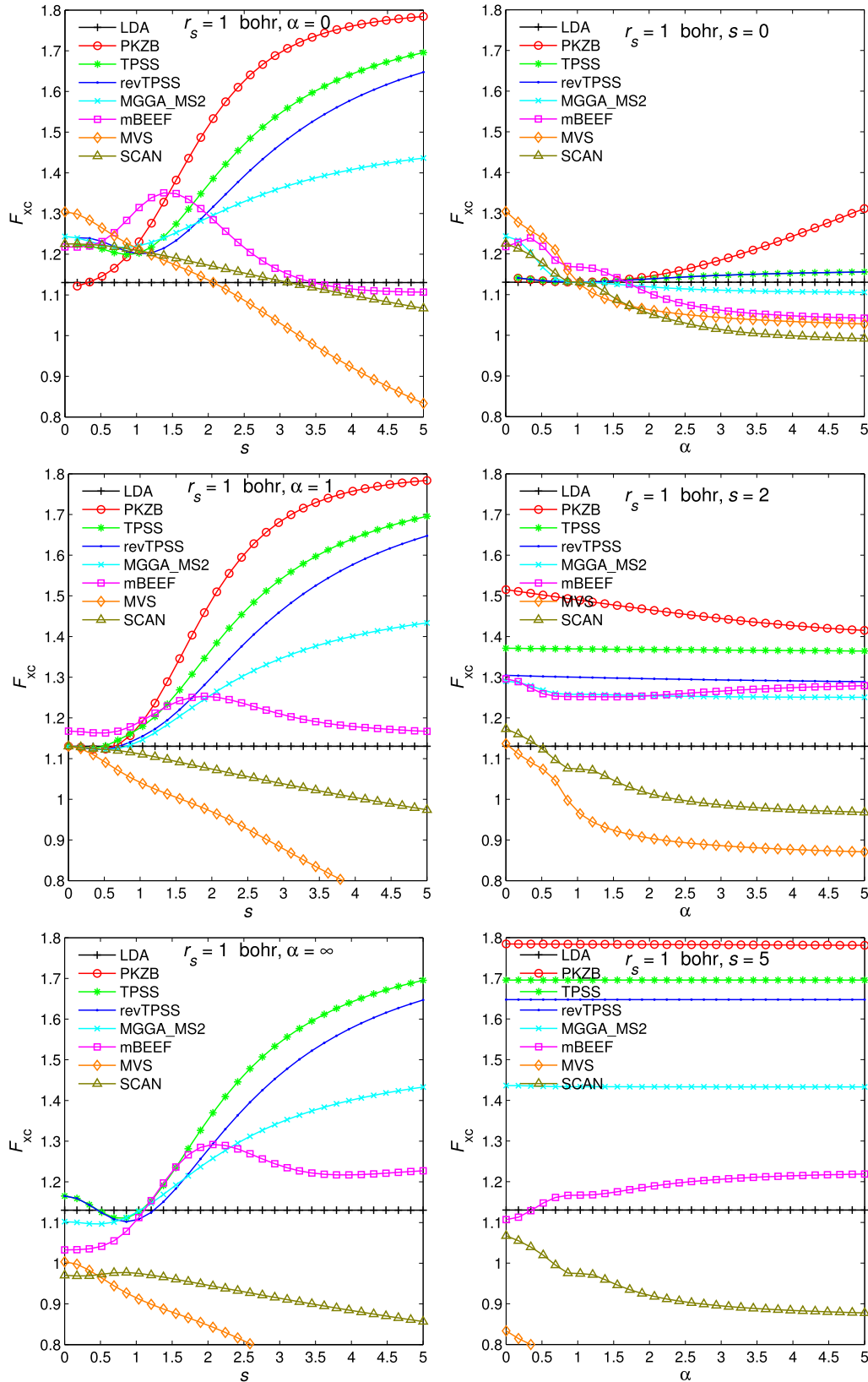


FIG. 2. MGGG enhancement factors F_{xc} plotted as a function of s for three values of α (left panels) and as a function of α for three values of s (right panels). r_s is kept fixed to 1 bohr. F_{xc} for LDA is also shown.

error (MARE), and maximum relative error (MAXRE) on the equilibrium lattice constant a_0 , bulk modulus B_0 , and cohesive energy E_{coh} for the 44 strongly bound solids. Most of the results are also shown graphically in Figs. 3 and 4, which provide

a convenient way to compare the performance of the functionals. The values of a_0 , B_0 , and E_{coh} for all solids and functionals can be found in the supplementary material.¹²⁶ Since the trends in the MRE/MARE are similar as for the ME/MAE,

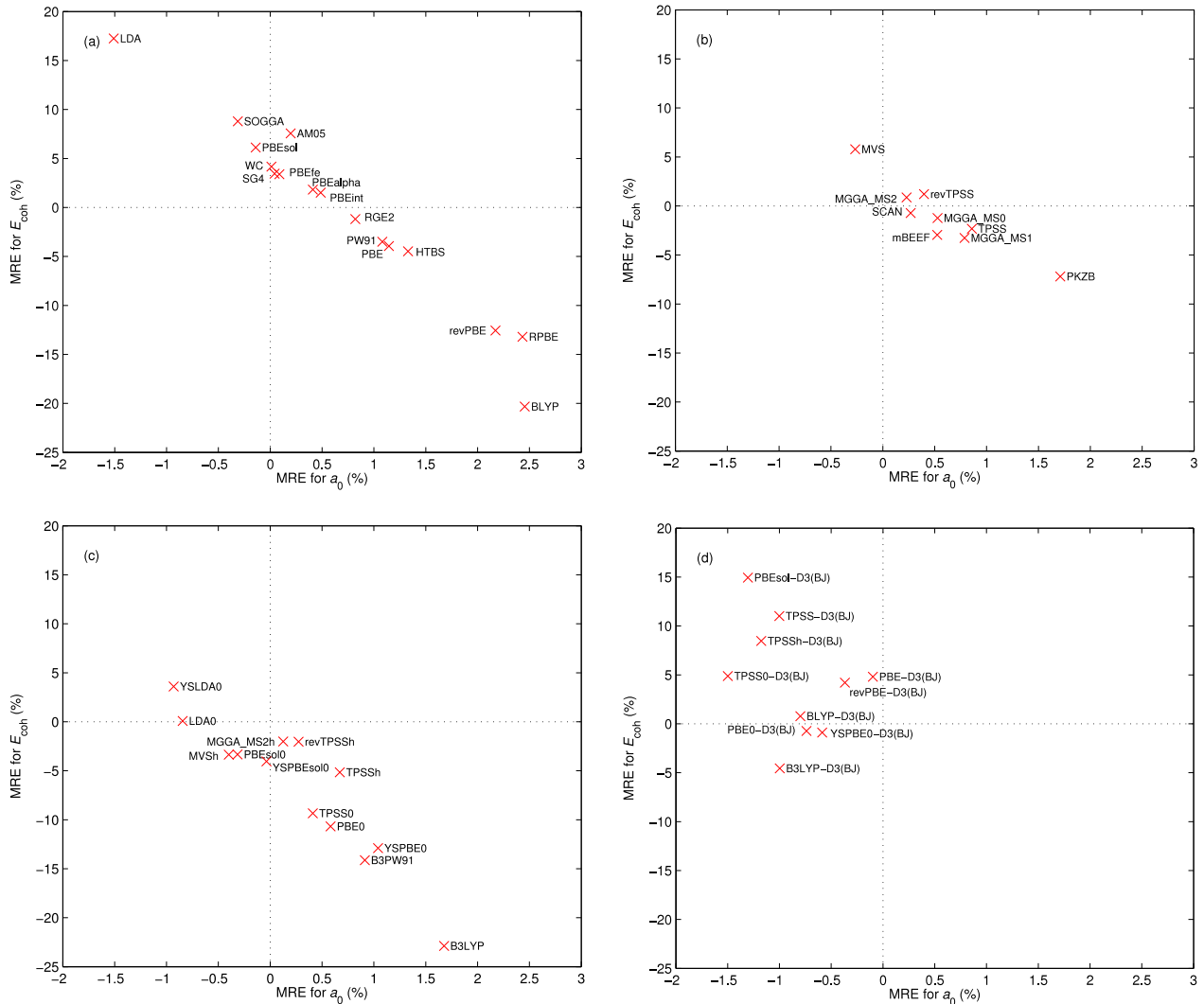


FIG. 3. MRE of a_0 versus MRE of E_{coh} for the (a) LDA and GGA, (b) MGGAs, (c) hybrid, and (d) DFT-D3(BJ) functionals.

the discussion of the results will be based mainly on the ME and MAE.

We start with the results for the lattice constant and bulk modulus. These two properties are quite often described with the same accuracy by a functional, but with opposite trends (i.e., an underestimation of a_0 is accompanied by an overestimation of B_0 or vice-versa), as seen in Figs. S1-S63 of the supplementary material¹²⁶ where the curves for the relative error for a_0 (left panel) and B_0 (middle panel) are approximately like mirror images. The smallest MAE for a_0 , 0.021 Å, is obtained by the hybrid-GGA functionals YSPBESol0 and PBEsol0, which is in-line with the conclusion of Ref. 43 that combining PBEsol with 25% of HF exchange improves over PBEsol (one of the most accurate GGA functionals for this quantity), PBE, and HSE06 (\approx YSPBE0). YSPBESol0 performs rather well also for B_0 with a MAE of 8.7 GPa, but is not the best method since a couple of other functionals lead to a MAE around 7.5 GPa, like for example WC, MGGA_MS2, SCAN, PBE0, and PBE-D3(BJ). Note that four functionals (PBEsol, MGGA_MS2, SCAN, and YSPBESol0) lead to a MARE for B_0 below 7%. The functionals which perform very well for both a_0 (MAE not larger than ~ 0.03 Å) and B_0 (MAE below 9 GPa) are the GGAs WC, SOGGA, PBEsol, and

SG4, the MGGAs MGGA_MS2 and SCAN, and the hybrids YSPBESol0 and MGGA_MS2h.

Turning now to the results for the cohesive energy E_{coh} , we can see that the MAE is below ~ 0.2 eV/atom for a dozen of functionals, e.g., the GGAs PW91, PBE, and PBEalpha, the MGGAs SCAN, the hybrid-MGGA revTPSSh, and a few DFT-D3/D3(BJ) methods. The MAE obtained with YSPBESol0 and PBEsol0 (the best for the lattice constant) is slightly larger (~ 0.27 eV/atom).

Overall, by considering the results for the three properties (a_0 , B_0 , and E_{coh}), the recent MGGAs MGGA_MS2 and SCAN seem to be the most accurate functionals. They are among the very best functionals for B_0 and E_{coh} , and only YSPBESol0, PBEsol0, and SG4 are more accurate for a_0 . Other functionals which are also consistently good for the three properties are the GGAs WC, PBEsol, PBEalpha, PBEint, and SG4, the hybrids YSPBESol0, MGGA_MS2h, and revTPSSh, and the dispersion-corrected PBE-D3 and PBE-D3(BJ).

It does not seem to be always necessary to use a functional with an atom-pairwise dispersion term [D3 or D3(BJ)] for the strongly bound solids. Actually, adding a dispersion term does not systematically improve the results (we remind that adding a dispersion term should, in principle, shorten bond

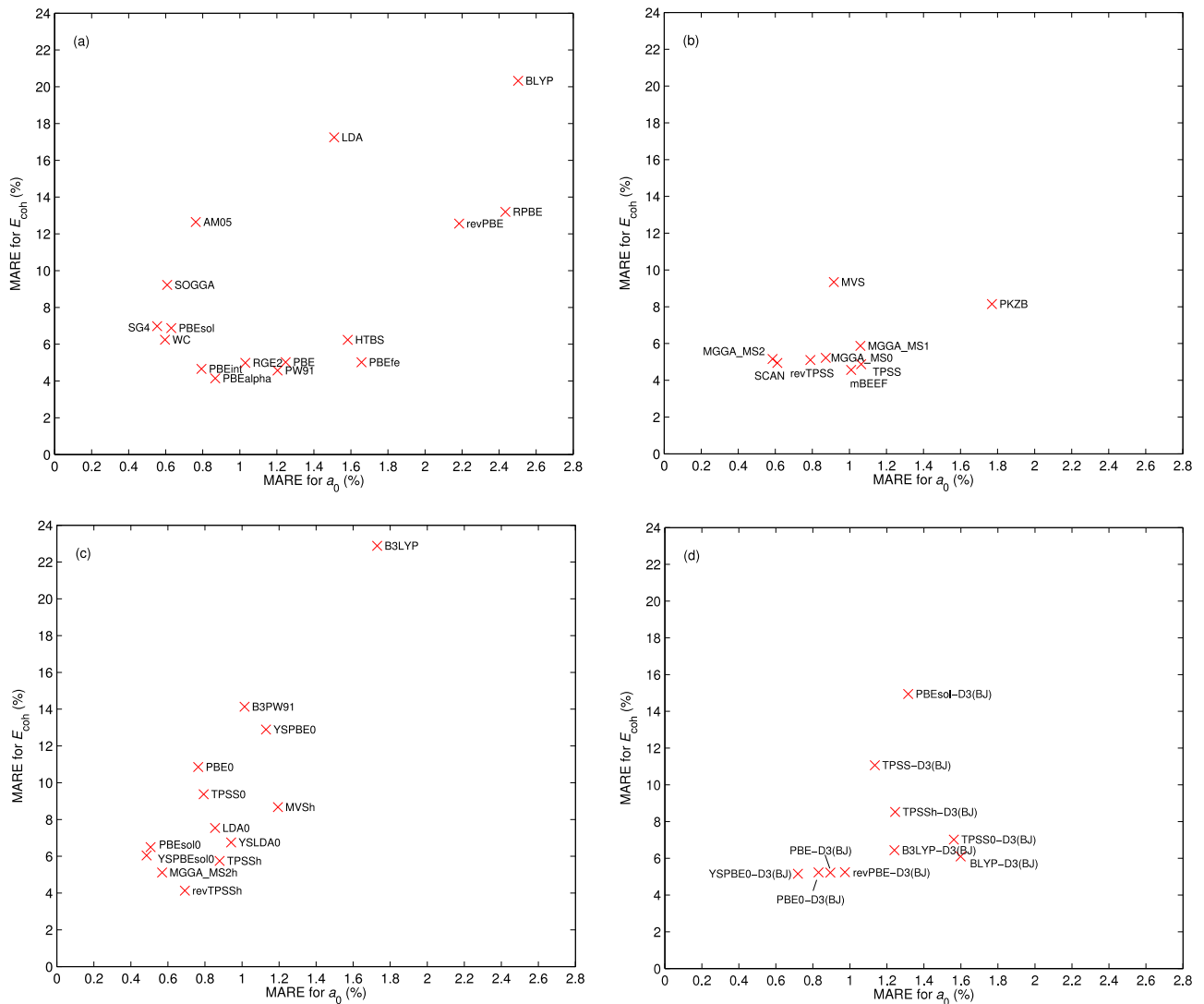


FIG. 4. MARE of a_0 versus MARE of E_{coh} for the (a) LDA and GGA, (b) MGGAs, (c) hybrid, and (d) DFT-D3(BJ) functionals.

lengths since the London dispersion interactions are attractive). This is, for instance, the case with TPSS, TPSSh, and TPSS0, for which the addition of D3(BJ) strongly overcorrects the overestimation of a_0 , leading to large negative ME (and large positive ME for B_0). In the case of PBEsol (very small ME for a_0 and B_0), adding D3 or D3(BJ) can only deteriorate the results since this functional alone does not overestimate the lattice constant on average. However, a clear improvement is obtained with PBE, revPBE, and BLYP. We note that none of these dispersion-corrected methods lead, for instance, to MAE below 0.040 Å for a_0 and 8 GPa for B_0 at the same time. Furthermore, the MAE for B_0 is rather large (above 10 GPa) for many of the dispersion corrected functionals, including PBE0-D3, which leads to a large MAE of 11.7 GPa despite its MAE for a_0 is only 0.027 Å. This shows that the curvature of the total-energy curve may not be described accurately by some of the DFT-D3/D3(BJ) functionals.

Regarding the hybrid functionals, it is instructive to look at how the MRE and MARE for a_0 and E_{coh} vary as functions of the fraction α_x of HF exchange in Eq. (2). This is shown in Fig. 5 for most screened and unscreened hybrid

functionals without D3 term, where α_x is varied between 0 and 0.5 with steps of 0.05. The trends observed in Fig. 5(a) for the MRE show two different behaviors. For the LDA-based and YSPBEsolh functionals, the value of the MRE for a_0 goes in the direction of the positive values when α_x is increased, while the opposite is observed with the other functionals. Interestingly, in most cases except PBEsolh and MVSh, adding a fraction of HF exchange reduces the magnitude of the MRE with respect to the case $\alpha_x = 0$. For the MARE [Fig. 5(b)], the main observations are the following: the smallest MARE for a_0 and E_{coh} is obtained simultaneously with more or less the same value of α_x in the case of PBEsolh, YSPBEsolh, revTPSSh, MGGA_MS2h, and SCANh. This optimal α_x is ~ 0 for MGGA_MS2h and SCANh and ~ 0.15 for the others. For MGGA_MS2h and SCANh, it can be argued that since MGGAs functionals are *more nonlocal* than LDA/GGA (in the sense that the KE density t is probably a truly nonlocal functional of ρ), then less HF exchange is required when combined with a MGGAs. For all other functionals except MVSh, the optimal α_x is larger for a_0 than for E_{coh} . The exception observed with MVSh should be related to the behavior of its enhancement

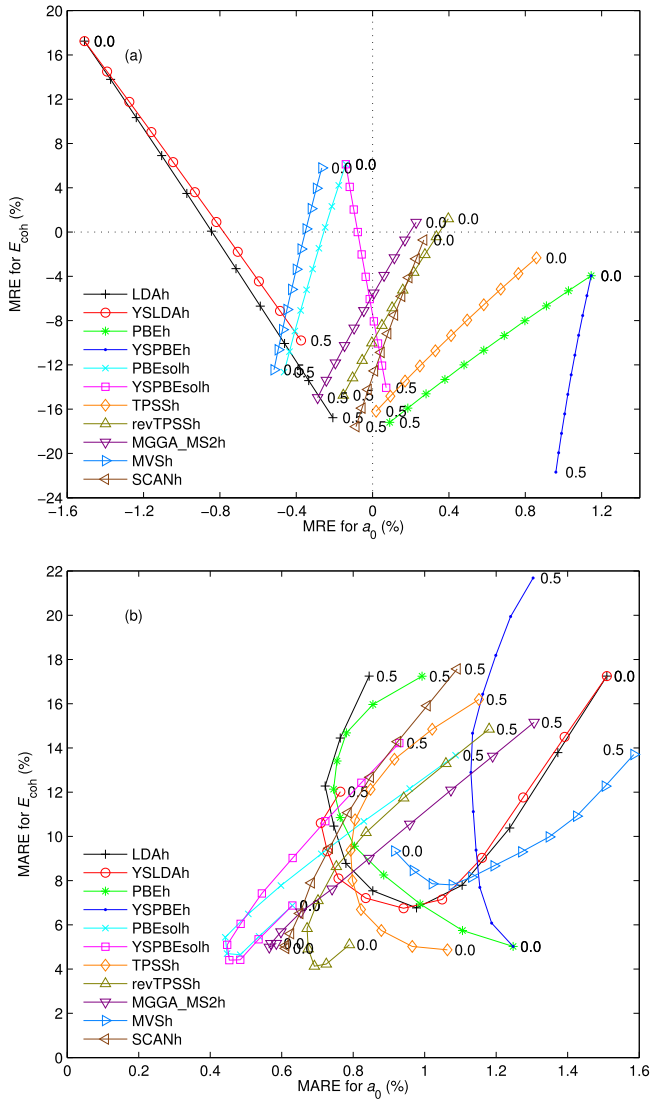


FIG. 5. (a) MRE of a_0 versus MRE of E_{coh} and (b) MARE of a_0 versus MARE of E_{coh} for hybrid functionals with the fraction of HF exchange α_x varied between 0 and 0.5 with steps of 0.05. The lines connecting the data points are guide to the eyes.

factor F_{xc} , which has by far the most negative slope as function of s and α , as noticed above in Fig. 2.

A few words about the functionals that were not considered in this work should also be added, and in particular about the so-called nonlocal van der Waals (vdW) functionals,²⁸ which include a term of the form given by Eq. (5). The first of these functionals which were shown to be, at least, as accurate as PBE for strongly bound solids, namely, optPBE-vdW, optB88-vdW, and optB86b-vdW, were proposed in Refs. 34 and 65. In Refs. 38, 40, 65, and 70, it was shown that compared to PBE, optB88-vdW and optPBE-vdW are slightly better for the cohesive energy, while optB86b-vdW is slightly better for the lattice constant. In order to make the SCAN functional more accurate for the treatment of weak interactions, Peng *et al.*¹²⁸ proposed to add a refitted version of the nonlocal vdW functional rVV10.^{31,32} For a test set of 50 solids, SCAN+rVV10 was shown to perform similarly as SCAN for the lattice constant, but to increase by about 1% the MARE for the cohesive energy.

The detailed results for every solid and functional are shown in the supplementary material,¹²⁶ and Fig. 6 gathers the results for some of the most accurate functionals compared to the standard PBE. In order to avoid a lengthy discussion, only the most interesting observations are now discussed. By looking at Figs. S1-S63,¹²⁶ which show the MRE (in %) for the lattice constant, bulk modulus, and cohesive energy, and the MAXRE in Table II, we can immediately see that for many functionals, some of the largest MRE for a_0 and B_0 is found for alkali metals (K, Rb, and Cs), alkali-earth metals (Ca, Sr, and Ba), and the transition metal V. For these solids, the MRE for a_0 increases with the nuclear charge and can reach 4%-8% for Cs. Such large MRE for a_0 is negative for LDA (accompanied by an overbinding) and positive (underbinding) for several GGAs like revPBE or HTBS and, quite interestingly, all (hybrid)-MGGAs. Such very large overestimations for the heavy alkali metals with TPSS and revTPSS were already reported.^{38,53,95,129} As argued in Ref. 129, the alkali metals are very soft (B_0 is below 5 GPa) and have a large polarizable core, such that the long-range core-core dispersion interactions, missing in non-dispersion corrected functionals, should have a non-negligible effect on the results. Therefore, it is maybe for the right reason that a semilocal/hybrid functional, in particular, if it is constructed from first-principles, underbinds the alkali metals. Adding a D3/D3(BJ) term reduces the error for the alkali metals, but overcorrects strongly in some cases [e.g., BLYP-D3(BJ) in Fig. S47¹²⁶]. The results with the DFT-D3/D3(BJ) methods could easily be improved by tuning the coefficients C_n^{AB} in Eq. (4). In the case of PBE-D3, for instance, it would be possible to strongly reduce the errors involving the Li atoms by using smaller value for the coefficients, while for all systems with the diamond or zincblende structures, larger coefficients would be required. On the other hand, as already mentioned in Sec. III, in the alkali metals, the value of s in the core-valence separation region is rather large,¹¹⁵ such that the shape of the enhancement factor at these large values of s maybe more important than for other solids. Such underbinding with the semilocal/hybrid functionals is not observed in the case of the similar alkali-earth metals, which should be due to the following reasons: they are slightly less van der Waals like (B_0 is above 10 GPa) and the additional valence s -electron should reduce the inhomogeneity in ρ , making the semilocal functionals more appropriate. The ionic solids LiX and NaX are systems for which the MRE can also be very large.

Looking at the trends for the 3d, 4d, and 5d transition metals, most functionals show the same behavior for the lattice constant; from left to right within a row (e.g., from Nb to Ag), the MRE goes in the direction of the positive values.^{38,51,63} This behavior is the most pronounced for the strong GGAs like revPBE or BLYP [also if D3/D3(BJ) is included], while it can be strongly reduced with some of the MGGa and hybrid functionals, similarly as RPA does.³⁸

A summary of this section on the strongly bound solids is the following. Among the tested functionals, about 12 of them are in the group of the best performing for all three properties (a_0 , B_0 , and E_{coh}) at the same time. This includes GGAs (WC, PBEsol, PBEalpha, PBEint, and SG4), MGGAs (MGGA_MS2 and SCAN), hybrids (YSPBEsol0,

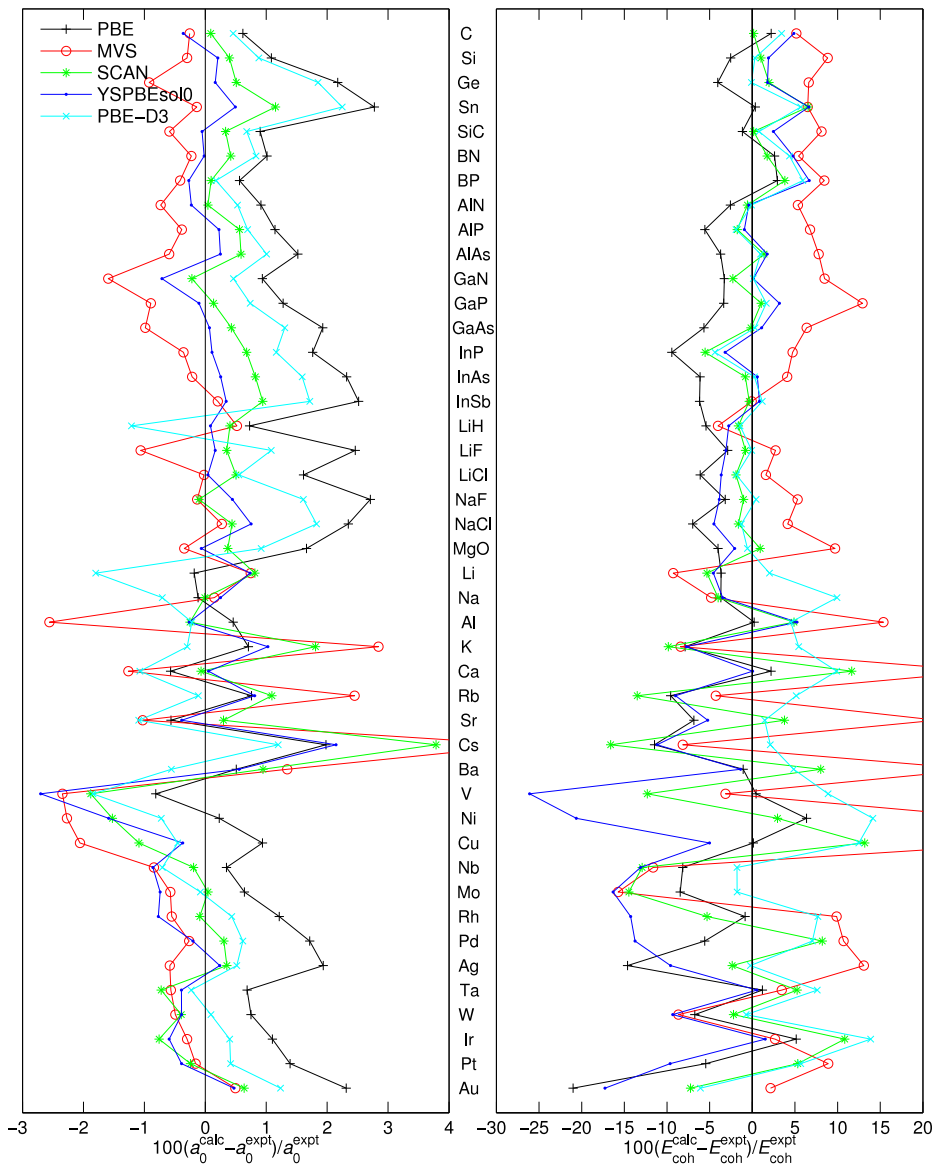


FIG. 6. Relative error (in %) in the calculated lattice constant (left panel) and cohesive energy (right panel) for the 44 strongly bound solids.

MGGA_MS2h, and revTPSSh), and dispersion-corrected methods [PBE-D3/D3(BJ)]. Therefore, as also shown more clearly in Figs. 3 and 4, for every type of approximations except LDA, there are a few functionals belonging to the group of the best ones. Furthermore, we have also noticed that MGGA_MS2 and SCAN give the best results when they are not mixed with HF exchange, which is a very interesting property from the practical point of view since the calculation of the HF exchange is very expensive for solids.

B. Weakly bound solids

In this section, the results for rare-gas solids (Ne, Ar, and Kr) and layered solids (graphite and h-BN) are discussed. Rare-gas dimers and solids, which are bound by the dispersion interactions, have been commonly used for the testing of theoretical methods (see Refs. 108, 130, 133, and 137–139 for the most recent works). The same is true for graphite and h-BN which are stacks of weakly bound hexagonal layers.^{66–68,79,132,135,140,141}

As mentioned in Sec. II, the results for such weakly bound systems are more sensitive to self-consistency effects than for the strongly bound solids. Figure 7 shows the example for Ar, where the MGGA_MS2 total-energy curves were obtained with four different sets of orbitals/density. Actually, this is a particularly bad case where the spread in the values for a_0 (5.4–5.7 Å) is two orders of magnitude larger than for most strongly bound solids and the spread for E_{coh} is of the same magnitude as E_{coh} itself. We observed that in general, the spread in a_0 is larger for functionals which lead to shallow minimum. This shows that there is some non-negligible degree of uncertainty in the results for the MGGA and hybrid functionals of Tables III and IV which were obtained non-self-consistently with PBE orbitals/density instead of self-consistently as it should be. Thus, for these functionals, the discussion should be kept at a qualitative level. On the other hand, the main conclusions of this section should not be affected too significantly, since for such weakly bound systems the errors with DFT functionals are often extremely large such that only the trends are usually discussed.

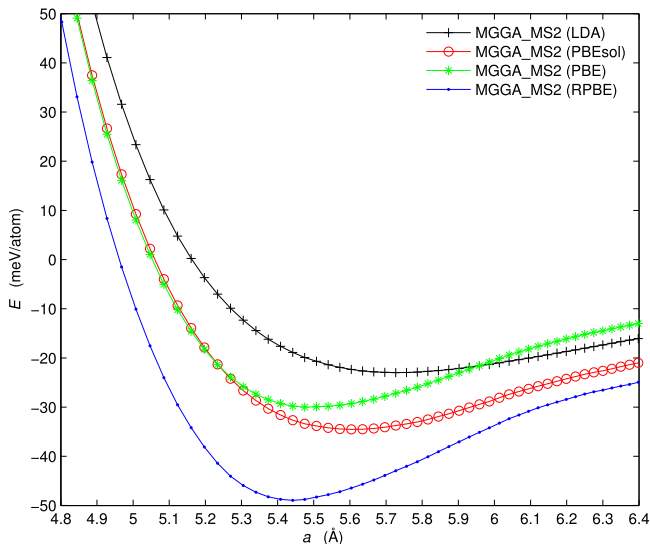


FIG. 7. MGGA_MS2 total energy of Ar plotted as a function of the lattice constant a . The MGGA_MS2 total-energy functional was evaluated with orbitals/densities generated from various potentials (indicated in parentheses). The zero of the energy axis was chosen such that the cohesive energy of Ar is given by the value at the minimum of a curve. The reference CCSD(T) values for a_0 and E_{coh} are 5.25 Å and 88 meV/atom, respectively.

1. Rare-gas solids

The results for the lattice constant and cohesive energy of the rare-gas solids are shown in Table III. The relative error (indicated in parentheses) is with respect to accurate results obtained from the CCSD(T) method.⁷⁷ Also shown are results taken from Refs. 14, 130, 133, and 134 that were obtained with nonlocal dispersion-corrected functionals [Eq. (5)], the atom-pairwise method of Tkatchenko and Scheffler,²⁶ and post-PBE RPA calculations. In a few cases, no minimum in the total-energy curve was obtained in the range of lattice constants that we have considered (largest values are 5.6, 6.6, 7.1 Å for Ne, Ar, Kr). This concerns the functionals revPBE, AM05, SG4, revTPSS(h), and those using B88 exchange (BLYP, B3LYP, and B3PW91). No minimum at all should exist with the B88-based functionals (see, e.g., Refs. 20 and 142–144), while only a very weak minimum at a larger lattice constant could eventually be expected with revPBE (see Ref. 145) and revTPSS (see Ref. 18). Note that no or a very weak binding is typically obtained by GGA functionals which violate the local Lieb-Oxford bound¹⁴⁶ because of an enhancement factor that is too large at large s ($s \geq 5$) like B88 and AM05 (see Fig. 1). The importance of the behavior of the enhancement factor at large s for noncovalent interactions was underlined in Refs. 147 and 148.

Unsurprisingly, the best functionals are those which include the atom-pairwise dispersion term D3/D3(BJ), since for many of them, the errors are below $\sim 8\%$ for a_0 and below $\sim 20\%$ for E_{coh} for all three rare gases. Such results are expected since the atom-dependent parameters in Eq. (4) (computed almost from first principles²⁷) should remain always accurate in the case of interaction between rare-gas atoms, whether it is in the dimer or in the solid. Note, however, that the error for the cohesive energy of Ne is above 100% for all MGGA_MS n (h)-D3 functionals, which may be due to the fact that only the term

$n = 6$ in Eq. (4) has been considered for these functionals.⁴⁶ All other functionals, without exception, lead to errors for E_{coh} which are above 50% for at least two rare gases. These large errors are always due to an underestimation for Ar and Kr, but not for Ne (overestimation with the MGGAs and underestimation with the others). For MGGA_MS2 and SCAN, the largest errors are -66% (Ar) and 107% (Ne), respectively. Note that the GGA PBEfe and MGGA mBEEF overestimate the cohesive energy even more than LDA does. For a_0 , the values obtained with the GGA PBEalpha and all modern (hybrid-)MGGAs like MGGA_MS2, SCAN, and mBEEF are in fair agreement with the CCSD(T) results since the errors are of the same order as with most dispersion-corrected functionals (below 8%).

Concerning previous works reporting tests on other functionals, we mention Ref. 130 where several variants of the nonlocal van der Waals functionals were tested on rare-gas dimers (from He₂ to Kr₂) and solids (Ne, Ar, and Kr). The conclusion was that rVV10^{31,32} leads to excellent results for the dimers and is among the good ones for the solids along with optB88-vdW³⁴ and C09x-vdW.¹³¹ However, with these three nonlocal functionals rather large errors in E_{coh} were still observed for the solids (results shown in Table III), such that overall these functionals are less accurate than DFT-D3/D3(BJ) for the rare-gas solids. Another nonlocal functional, rev-vdW-DF2, was recently proposed by Hamada,¹³² and the results on rare-gas solids¹³³ (see Table III) are as good as the DFT-D3/D3(BJ) results and, therefore, better than for the other three nonlocal functionals. For the Ar and Kr dimers, the SCAN+rVV10 functional was shown to be as accurate as rVV10,¹²⁸ however it has not been tested on rare-gas solids. Finally, we also mention the RPA (fifth rung of Jacob's ladder) results from Ref. 14 which are rather accurate overall, as shown in Table III. Concerning other semilocal approximations not augmented with a dispersion correction, previous works reported unsuccessful attempts to find such a functional leading to accurate results for all rare-gas dimers at the same time (see, e.g., Refs. 144 and 149).

The summary for the rare-gas solids is the following. For the cohesive energy, the functionals which include an atom-pairwise term D3/D3(BJ) clearly outperform the others. It was also observed that the MGGAs do not improve over the GGAs for E_{coh} . However, for the lattice constant, MGGAs are superior to the GGAs and perform as well as the dispersion corrected-functionals. Among the previous works also considering rare-gas solids in their test set, we noted that the rev-vdW-DF2 nonlocal functional^{132,133} shows similar accuracy as the DFT-D3/D3(BJ) methods.

2. Layered solids

Turning now to the layered solids graphite and h-BN, the results for the equilibrium lattice constant c_0 (the interlayer distance is $c_0/2$) and interlayer binding energy E_b are shown in Table IV. Since for these two systems we are interested only in the interlayer properties, the intralayer lattice constant a was kept fixed at the experimental value of 2.462 and 2.503 Å for graphite and h-BN, respectively. As in the recent works of Björkman *et al.*,^{66–68,79} the results from the RPA

TABLE III. Equilibrium lattice constant a_0 (in Å) and cohesive energy E_{coh} (in meV/atom and with opposite sign) of rare-gas solids calculated from various functionals and compared to reference [CCSD(T), very close to experiment] as well as other methods. The results for the LDA, GGA, and GGA+D functionals were obtained from self-consistent calculations, while the PBE orbitals/density were used for the other functionals. Within each group, the functionals are ordered by increasing overall error. For hybrid functionals, the fraction α_x of HF exchange is indicated in parentheses.

Functional	Ne		Ar		Kr	
	a_0	E_{coh}	a_0	E_{coh}	a_0	E_{coh}
LDA						
LDA ⁸⁰	3.86 (−10%)	87 (234%)	4.94 (−6%)	138 (57%)	5.33 (−5%)	169 (39%)
GGA						
PBEalpha ⁸⁶	4.39 (2%)	23 (−10%)	5.59 (6%)	33 (−62%)	5.97 (7%)	43 (−65%)
SOGGA ⁸²	4.52 (5%)	23 (−11%)	5.77 (10%)	29 (−67%)	6.14 (10%)	35 (−71%)
RPBE ⁹²	4.74 (10%)	26 (0%)	6.25 (19%)	28 (−68%)	6.83 (22%)	29 (−76%)
PBE ⁷³	4.60 (7%)	19 (−26%)	5.96 (13%)	23 (−73%)	6.42 (15%)	27 (−78%)
HTBS ⁸⁹	4.80 (12%)	23 (−12%)	6.34 (21%)	25 (−72%)	6.93 (24%)	26 (−79%)
PW91 ⁸⁸	4.62 (7%)	47 (82%)	6.05 (15%)	49 (−44%)	6.55 (17%)	51 (−58%)
PBEsol ⁸³	4.70 (9%)	12 (−54%)	5.88 (12%)	17 (−81%)	6.13 (10%)	23 (−81%)
PBEint ⁸⁵	4.78 (11%)	14 (−46%)	6.21 (18%)	17 (−81%)	6.67 (19%)	20 (−84%)
RGE2 ⁸⁷	4.92 (14%)	14 (−45%)	6.43 (23%)	16 (−81%)	6.99 (25%)	18 (−85%)
WC ⁸¹	4.87 (13%)	12 (−54%)	6.34 (21%)	14 (−84%)	6.86 (23%)	16 (−87%)
PBEfe ⁹⁰	3.88 (−10%)	99 (280%)	5.00 (−5%)	152 (73%)	5.42 (−3%)	184 (51%)
SG4 ⁶⁰	5.25 (22%)	9 (−67%)	>6.6 (>26%)		>7.1 (>27%)	
revPBE ⁹¹	5.31 (24%)	7 (−74%)	>6.6 (>26%)		>7.1 (>27%)	
BLYP ^{93,94}	>5.6 (>31%)		>6.6 (>26%)		>7.1 (>27%)	
AM05 ⁸⁴	>5.6 (>31%)		>6.6 (>26%)		>7.1 (>27%)	
MGGA						
MGGA_MS2 ⁴⁶	4.31 (0%)	26 (1%)	5.48 (4%)	30 (−66%)	5.96 (6%)	45 (−63%)
MGGA_MS1 ⁴⁶	4.34 (1%)	26 (0%)	5.58 (6%)	27 (−69%)	6.10 (9%)	40 (−67%)
MGGA_MS0 ⁴⁵	4.16 (−3%)	40 (53%)	5.41 (3%)	46 (−47%)	5.89 (5%)	61 (−50%)
SCAN ⁴⁸	4.03 (−6%)	54 (107%)	5.31 (1%)	61 (−30%)	5.74 (2%)	72 (−41%)
PKZB ⁹⁷	4.66 (9%)	27 (2%)	6.20 (18%)	26 (−70%)	6.76 (21%)	30 (−75%)
MVS ⁴⁷	4.02 (−6%)	59 (125%)	5.41 (3%)	56 (−37%)	5.79 (3%)	69 (−43%)
TPSS ⁹⁶	4.92 (15%)	11 (−59%)	6.45 (23%)	11 (−87%)	6.98 (25%)	15 (−88%)
mBEEF ⁴⁹	3.92 (−9%)	134 (416%)	5.26 (0%)	142 (62%)	5.75 (3%)	161 (32%)
revTPSS ⁹⁵	5.05 (17%)	7 (−72%)	>6.6 (>26%)		7.04 (26%)	12 (−90%)
hybrid-LDA						
LDA0 ^{80,98} (0.25)	4.00 (−7%)	51 (96%)	5.18 (−1%)	71 (−19%)	5.57 (0%)	90 (−26%)
YSLDA0 ^{80,98} (0.25)	3.96 (−8%)	60 (131%)	5.12 (−2%)	86 (−2%)	5.51 (−1%)	108 (−11%)
hybrid-GGA						
PBE0 ^{99,100} (0.25)	4.61 (7%)	11 (−57%)	5.96 (14%)	15 (−83%)	6.41 (15%)	19 (−84%)
PBEsol0 ^{83,98} (0.25)	4.66 (8%)	7 (−75%)	5.79 (10%)	12 (−86%)	6.06 (8%)	20 (−84%)
YSPBE0 ^{74,101} (0.25)	4.76 (11%)	10 (−60%)	6.21 (18%)	14 (−84%)	6.69 (19%)	17 (−86%)
YSPBEsol0 ⁴³ (0.25)	4.93 (15%)	5 (−81%)	6.26 (19%)	8 (−91%)	6.55 (17%)	11 (−91%)
B3LYP ¹⁰² (0.20)	>5.6 (>31%)		>6.6 (>26%)		>7.1 (>27%)	
B3PW91 ¹¹ (0.20)	>5.6 (>31%)		>6.6 (>26%)		>7.1 (>27%)	
hybrid-MGGA						
MGGA_MS2h ⁴⁶ (0.09)	4.31 (0%)	23 (−11%)	5.48 (4%)	27 (−70%)	5.97 (7%)	41 (−67%)
MVSh ⁴⁷ (0.25)	4.05 (−6%)	40 (55%)	5.44 (4%)	40 (−55%)	5.83 (4%)	52 (−58%)
TPSSh ¹⁰⁴ (0.10)	4.93 (15%)	8 (−67%)	6.46 (23%)	9 (−90%)	6.98 (25%)	13 (−90%)
TPSS0 ^{96,98} (0.25)	4.96 (15%)	5 (−80%)	6.47 (23%)	6 (−93%)	6.98 (25%)	9 (−92%)
revTPSSh ¹⁰³ (0.10)	5.06 (18%)	5 (−79%)	>6.6 (>26%)		7.03 (26%)	10 (−92%)
GGA+D						
revPBE-D3(BJ) ¹⁰⁶	4.80 (12%)	25 (−2%)	5.67 (8%)	82 (−7%)	5.96 (7%)	126 (3%)
PBEsol-D3(BJ) ¹⁰⁵	4.59 (7%)	22 (−16%)	5.46 (4%)	71 (−19%)	5.69 (2%)	116 (−5%)
revPBE-D3 ²⁷	4.73 (10%)	25 (−4%)	5.64 (7%)	68 (−23%)	5.85 (5%)	109 (−11%)
PBE-D3(BJ) ¹⁰⁶	4.46 (4%)	37 (42%)	5.49 (5%)	86 (−2%)	5.85 (5%)	117 (−4%)
PBEsol-D3 ¹⁰⁵	4.53 (5%)	29 (13%)	5.37 (2%)	61 (−31%)	5.58 (0%)	102 (−17%)
BLYP-D3 ²⁷	4.25 (−1%)	16 (−38%)	5.35 (2%)	70 (−21%)	5.70 (2%)	127 (4%)

TABLE III. (Continued.)

Functional	Ne		Ar		Kr	
	a_0	E_{coh}	a_0	E_{coh}	a_0	E_{coh}
PBE-D3 ²⁷	4.39 (2%)	46 (78%)	5.58 (6%)	83 (-6%)	5.90 (5%)	113 (-8%)
BLYP-D3(BJ) ¹⁰⁶	4.58 (7%)	3 (-89%)	5.37 (2%)	71 (-19%)	5.67 (1%)	134 (10%)
RPBE-D3 ¹⁰⁷	4.49 (4%)	52 (101%)	5.66 (8%)	91 (3%)	6.03 (8%)	116 (-5%)
MGGA+D						
TPSS-D3(BJ) ¹⁰⁶	4.69 (9%)	28 (7%)	5.67 (8%)	78 (-11%)	5.97 (7%)	118 (-3%)
TPSS-D3 ²⁷	4.53 (6%)	36 (39%)	5.69 (8%)	76 (-14%)	5.99 (7%)	111 (-9%)
MGGA_MS2-D3 ⁴⁶	4.19 (-3%)	55 (113%)	5.43 (3%)	83 (-6%)	5.91 (5%)	105 (-14%)
MGGA_MS1-D3 ⁴⁶	4.14 (-4%)	60 (132%)	5.37 (2%)	96 (9%)	5.83 (4%)	121 (-1%)
MGGA_MS0-D3 ⁴⁶	4.10 (-5%)	70 (170%)	5.38 (2%)	98 (11%)	5.85 (4%)	120 (-2%)
hybrid-GGA+D						
PBE0-D3(BJ) ¹⁰⁶ (0.25)	4.45 (4%)	28 (7%)	5.46 (4%)	82 (-7%)	5.79 (3%)	121 (-1%)
B3LYP-D3 ²⁷ (0.20)	4.25 (-1%)	23 (-10%)	5.30 (1%)	68 (-23%)	5.61 (0%)	129 (5%)
YSPBE0-D3(BJ) ¹⁰⁸ (0.25)	4.62 (8%)	23 (-11%)	5.66 (8%)	75 (-15%)	5.98 (7%)	116 (-5%)
PBE0-D3 ²⁷ (0.25)	4.39 (2%)	36 (40%)	5.45 (4%)	74 (-16%)	5.71 (2%)	114 (-6%)
B3LYP-D3(BJ) ¹⁰⁶ (0.20)	4.39 (2%)	12 (-52%)	5.32 (1%)	78 (-12%)	5.65 (1%)	135 (11%)
YSPBE0-D3 ¹⁰⁷ (0.25)	4.46 (4%)	33 (25%)	5.75 (9%)	60 (-32%)	6.21 (11%)	74 (-39%)
hybrid-MGGA+D						
TPSSh-D3(BJ) ¹⁰⁹ (0.10)	4.69 (9%)	25 (-3%)	5.65 (8%)	79 (-10%)	5.94 (6%)	122 (0%)
TPSS0-D3 ²⁷ (0.25)	4.53 (5%)	29 (13%)	5.64 (7%)	66 (-25%)	5.78 (3%)	108 (-12%)
TPSS0-D3(BJ) ¹⁰⁶ (0.25)	4.66 (8%)	21 (-18%)	5.57 (6%)	70 (-21%)	5.81 (4%)	112 (-8%)
TPSSh-D3 ¹⁰⁵ (0.10)	4.55 (6%)	33 (28%)	5.70 (9%)	70 (-20%)	5.91 (6%)	108 (-12%)
MGGA_MS2h-D3 ⁴⁶ (0.09)	4.18 (-3%)	52 (100%)	5.44 (4%)	79 (-10%)	5.91 (5%)	101 (-17%)
Previous works						
optB88-vdW ³⁴ (Ref. 130)	4.24 (-1%)	59 (127%)	5.24 (0%)	143 (62%)	5.63 (1%)	181 (48%)
C09x-vdW ¹³¹ (Ref. 130)	4.50 (5%)	62 (138%)	5.33 (2%)	128 (45%)	5.64 (1%)	163 (34%)
rVV10 ^{31,32} (Ref. 130)	4.19 (-2%)	49 (88%)	5.17 (-2%)	117 (33%)	5.53 (-1%)	162 (33%)
rev-vdW-DF2 ¹³² (Ref. 133)	4.43 (3%)	30 (15%)	5.35 (2%)	90 (2%)	5.71 (2%)	120 (-2%)
PBE+TS ²⁶ (Ref. 134)	4.42 (3%)	43 (65%)	5.51 (5%)	83 (-6%)	5.90 (5%)	97 (-20%)
RPA (Ref. 14)	4.5 (5%)	17 (-35%)	5.3 (1%)	83 (-6%)	5.7 (2%)	112 (-8%)
Expt. (Ref. 77)	4.29	26	5.25	88	5.63	122
CCSD(T) (Ref. 77)	4.30	26	5.25	88	5.60	122

method,^{78,79} which are in very good agreement with experiment and Monte Carlo simulation¹⁵⁰ for graphite, are used as reference. No experimental result for E_b for h-BN seems to be available.

The results with the GGA functionals are extremely inaccurate since for all these methods, except PBEfe, there is no or a very tiny binding between the layers (underestimation of E_b by more than 90%) and a huge overestimation of c_0 by at least 0.5 Å. The underestimation of E_b with PBEfe is ~50% and c_0 is too large by ~0.3 Å. LDA also underestimates E_b by ~40%, but leads to interlayer distances which agree quite well with RPA and, actually, perfectly for graphite. The best MGGA functional is MVS, whose relative error is -34% for the binding energy of graphite, but below 5% otherwise. SCAN performs slightly worse since E_b is too small by ~50% for both graphite and h-BN, while MGGA_MS2 leads to disappointingly small binding energies. The other MGGA, including mBEEF, lead to very small (large) values for E_b (c_0). Note that the results obtained with mBEEF show totally different trends as those for the rare gases (large overbinding for the rare gases and large underbinding for

graphite and h-BN), which is maybe due to the nonsmooth form of this functional (see Fig. 2) such that the results are more unpredictable. Among the hybrid functionals, MVSh is the only one which leads to somehow reasonable results, with errors for E_b that are slightly larger than for the underlying semilocal MVS. Let us remark that all functionals without dispersion correction underestimate the interlayer binding energy of graphite and h-BN, while it was not the case for the cohesive energy of the rare-gas solids.

Adding the D3 or D3(BJ) dispersion term usually improves the agreement with RPA, such that for many of these methods, the magnitude of the relative error is below 20% and 3% for E_b and c_0 , respectively. Such errors can be considered as relatively modest. Among the computationally cheap GGA+D, the accurate functionals are PBE-D3/D3(BJ), RPBE-D3, and PBEsol-D3.

The results obtained with many other methods are available in the literature^{66-68,79,132,135,140,141} (see Ref. 141 for a collection of values for graphite), and those obtained from the methods that were already selected for the discussion on the rare gases are shown in Table IV. The nonlocal functionals

TABLE IV. Equilibrium lattice constant c_0 (in Å) and interlayer binding energy E_b (in meV/atom and with opposite sign) of layered solids calculated from various functionals and compared to reference (RPA) as well as other methods. The results for the LDA, GGA, and GGA+D functionals were obtained from self-consistent calculations, while the PBE orbitals/density were used for the other functionals. Within each group, the functionals are ordered by increasing overall error. For hybrid functionals, the fraction α_x of HF exchange is indicated in parentheses. The results for the DFT-D3/D3(BJ) functionals without the three-body term can be found in Table S22 of the supplementary material.¹²⁶

Functional	Graphite		h-BN	
	c_0	E_b	c_0	E_b
LDA				
LDA ⁸⁰	6.7 (0%)	24 (-50%)	6.5 (-3%)	28 (-28%)
GGA				
PBE _{fe} ⁹⁰	7.0 (5%)	21 (-57%)	6.9 (3%)	24 (-39%)
SOGGA ⁸²	7.3 (9%)	4 (-91%)	7.0 (5%)	7 (-83%)
PBEsol ⁸³	7.3 (9%)	4 (-92%)	7.0 (6%)	6 (-84%)
PBEalpha ⁸⁶	7.6 (14%)	4 (-91%)	7.3 (10%)	6 (-84%)
PBE ⁷³	~8.8 (31%)	1 (-97%)	~8.5 (28%)	2 (-94%)
PW91 ⁸⁸	~9.3 (38%)	2 (-95%)	~9.0 (36%)	3 (-93%)
PBEint ⁸⁵	~9.3 (39%)	1 (-98%)	~9.0 (35%)	2 (-96%)
WC ⁸¹	~9.7 (45%)	1 (-99%)	~9.5 (42%)	1 (-97%)
RPBE ⁹²	~9.8 (46%)	1 (-97%)	~9.8 (47%)	2 (-96%)
HTBS ⁸⁹	~9.9 (48%)	1 (-98%)	~9.9 (49%)	2 (-96%)
RGE2 ⁸⁷	~10.0 (49%)	1 (-99%)	~10.0 (49%)	1 (-97%)
SG4 ⁶⁰	~11.0 (64%)	0 (-99%)	~11.0 (65%)	1 (-98%)
revPBE ⁹¹	~11.3 (69%)	0 (-99%)	~11.3 (70%)	1 (-98%)
AM05 ⁸⁴	>19 (>176%)		>19 (>188%)	
BLYP ^{93,94}	>19 (>176%)		>19 (>188%)	
MGGA				
MVS ⁴⁷	6.6 (-1%)	32 (-34%)	6.4 (-4%)	38 (-4%)
SCAN ⁴⁸	6.9 (3%)	20 (-59%)	6.8 (2%)	21 (-46%)
mBEEF ⁴⁹	7.8 (16%)	13 (-72%)	7.7 (16%)	14 (-63%)
MGGA_MS2 ⁴⁶	7.2 (7%)	8 (-83%)	7.0 (5%)	10 (-74%)
MGGA_MS0 ⁴⁵	7.4 (11%)	8 (-83%)	7.3 (9%)	9 (-76%)
MGGA_MS1 ⁴⁶	7.8 (16%)	5 (-90%)	7.7 (16%)	6 (-86%)
PKZB ⁹⁷	7.9 (19%)	4 (-91%)	7.9 (18%)	5 (-88%)
revTPSS ⁹⁵	>19 (>176%)		~9.8 (47%)	1 (-98%)
TPSS ⁹⁶	>19 (>176%)		~9.9 (49%)	1 (-98%)
hybrid-LDA				
YSLDA0 ^{80,98} (0.25)	7.0 (4%)	15 (-70%)	6.7 (1%)	18 (-53%)
LDA0 ^{80,98} (0.25)	7.1 (5%)	12 (-74%)	6.8 (2%)	16 (-60%)
hybrid-GGA				
PBEsol0 ^{83,98} (0.25)	7.3 (9%)	5 (-90%)	7.0 (5%)	7 (-81%)
YSPBEsol0 ⁴³ (0.25)	~7.8 (17%)	1 (-97%)	~7.3 (10%)	3 (-92%)
PBE0 ^{99,100} (0.25)	~8.4 (25%)	2 (-97%)	~8.0 (20%)	3 (-94%)
YSPBE0 ^{74,101} (0.25)	~9.3 (39%)	1 (-98%)	~9.0 (36%)	1 (-97%)
B3LYP ¹⁰² (0.20)	>19 (>176%)		>19 (>188%)	
B3PW91 ¹¹ (0.20)	>19 (>176%)		>19 (>188%)	
hybrid-MGGA				
MVSh ⁴⁷ (0.25)	6.7 (0%)	25 (-48%)	6.5 (-3%)	31 (-22%)
MGGA_MS2h ⁴⁶ (0.09)	7.2 (7%)	8 (-83%)	7.0 (5%)	10 (-74%)
revTPSSh ¹⁰³ (0.10)	>19 (>176%)		~9.4 (41%)	1 (-98%)
TPSSh ¹⁰⁴ (0.10)	>19 (>176%)		~9.8 (48%)	1 (-98%)
TPSS0 ^{96,98} (0.25)	>19 (>176%)		~9.6 (44%)	1 (-98%)
GGA+D				
RPBE-D3 ¹⁰⁷	6.8 (1%)	39 (-19%)	6.7 (0%)	39 (0%)
PBE-D3(BJ) ¹⁰⁶	6.8 (2%)	43 (-10%)	6.7 (0%)	44 (12%)
PBEsol-D3 ¹⁰⁵	6.7 (0%)	38 (-20%)	6.6 (-2%)	42 (8%)

TABLE IV. (Continued.)

Functional	Graphite		h-BN	
	c_0	E_b	c_0	E_b
PBE-D3 ²⁷	7.1 (5%)	39 (-19%)	6.8 (3%)	41 (5%)
PBEsol-D3(BJ) ¹⁰⁵	6.7 (-1%)	52 (8%)	6.5 (-3%)	53 (36%)
revPBE-D3 ²⁷	6.6 (-2%)	53 (10%)	6.5 (-2%)	52 (33%)
BLYP-D3 ²⁷	6.8 (1%)	59 (22%)	6.7 (0%)	58 (49%)
revPBE-D3(BJ) ¹⁰⁶	6.5 (-4%)	67 (41%)	6.3 (-5%)	69 (77%)
BLYP-D3(BJ) ¹⁰⁶	6.6 (-2%)	70 (46%)	6.5 (-3%)	71 (83%)
MGGA+D				
MGGA_MS1-D3 ⁴⁶	6.9 (2%)	46 (-4%)	6.8 (2%)	44 (12%)
MGGA_MS2-D3 ⁴⁶	6.8 (2%)	45 (-6%)	6.6 (-1%)	46 (17%)
MGGA_MS0-D3 ⁴⁶	7.0 (5%)	42 (-13%)	6.8 (3%)	42 (7%)
TPSS-D3 ²⁷	6.7 (0%)	47 (-1%)	6.5 (-2%)	50 (28%)
TPSS-D3(BJ) ¹⁰⁶	6.5 (-3%)	58 (21%)	6.3 (-5%)	60 (53%)
hybrid-GGA+D				
YSPBE0-D3(BJ) ¹⁰⁸ (0.25)	7.0 (4%)	46 (-5%)	6.8 (2%)	46 (19%)
PBE0-D3 ²⁷ (0.25)	6.9 (2%)	41 (-14%)	6.7 (0%)	45 (16%)
PBE0-D3(BJ) ¹⁰⁶ (0.25)	6.7 (0%)	50 (3%)	6.5 (-2%)	51 (31%)
B3LYP-D3 ²⁷ (0.20)	6.8 (2%)	50 (5%)	6.7 (1%)	54 (38%)
YSPBE0-D3 ¹⁰⁷ (0.25)	7.3 (9%)	30 (-36%)	7.1 (6%)	30 (-23%)
B3LYP-D3(BJ) ¹⁰⁶ (0.20)	6.7 (-1%)	62 (29%)	6.5 (-3%)	64 (64%)
hybrid-MGGA+D				
MGGA_MS2h-D3 ⁴⁶ (0.09)	6.8 (2%)	45 (-7%)	6.6 (-1%)	46 (18%)
TPSSh-D3 ¹⁰⁵ (0.10)	6.7 (0%)	47 (-2%)	6.5 (-2%)	51 (30%)
TPSS0-D3 ²⁷ (0.25)	6.6 (-1%)	48 (0%)	6.5 (-3%)	53 (35%)
TPSS0-D3(BJ) ¹⁰⁶ (0.25)	6.5 (-3%)	56 (17%)	6.2 (-6%)	60 (54%)
TPSSh-D3(BJ) ¹⁰⁹ (0.10)	6.5 (-3%)	61 (28%)	6.3 (-5%)	63 (62%)
Previous works				
optB88-vdW ³⁴ (Ref. 68)	6.76 (1%)	66 (38%)	6.64 (1%)	67 (72%)
C09x-vdW ¹³¹ (Ref. 68)	6.54 (-2%)	71 (48%)	6.42 (-3%)	73 (87%)
VV10 ^{31,32} (Ref. 67)	6.68 (0%)	71 (48%)	6.57 (0%)	70 (79%)
rev-vdW-DF2 ¹³² (Ref. 132)	6.64 (-1%)	60 (25%)	6.56 (-1%)	57 (46%)
PW86R-VV10sol ⁶⁷ (Ref. 67)	6.98 (5%)	44 (-8%)	6.87 (4%)	43 (10%)
AM05-VV10sol ⁶⁷ (Ref. 67)	6.99 (5%)	45 (-6%)	6.84 (4%)	41 (5%)
PBE+TS ²⁶ (Ref. 135)	6.68 (0%)	82 (71%)	6.64 (1%)	87 (123%)
PBE+TS+SCS ¹³⁶ (Ref. 135)	6.75 (1%)	55 (15%)	6.67 (1%)	73 (87%)
RPA (Refs. 78 and 79)	6.68	48	6.60	39

optB88-vdW, C09x-vdW, VV10, and rev-vdW-DF2 as well as PBE+TS(+SCS) lead to very good agreement with RPA for the interlayer lattice constant (errors in the range 0%-2%); however, in most cases there is a non-negligible overbinding above 40%. Also shown in Table IV are the results obtained with the nonlocal functionals PW86R-VV10sol and AM05-VV10sol which contain parameters that were fitted specifically to RPA binding energies of 26 layered solids including graphite and h-BN.⁶⁷ Unsurprisingly, the errors obtained with PW86R-VV10sol and AM05-VV10sol for E_b are very small (below 10%), but the price to pay are errors for c_0 that are clearly larger (~5%) than with the other nonlocal functionals. The nonlocal functional SCAN+rVV10 has also been tested on a set of 28 layered solids, and according to Ref. 128, the MARE (the detailed results for each system are not available) for the interlayer lattice constant and binding energy amounts to 1.5% and 7.7%, respectively, meaning that SCAN+rVV10

leads to very low errors for both quantities, despite no parameter was tuned to reproduce the results for the layered solids.

In summary, among the methods which do not include an atom-pairwise dispersion correction, only a couple of them (MVS, LDA, and PBEfe) do not severely underestimate the interlayer binding energy. Adding a D3/D3(BJ) atom-pairwise term clearly improves the results, leading to rather satisfying values for the interlayer spacing and binding energy. In the group of nonlocal functionals, the recently proposed SCAN+rVV10 seems to be among the most accurate.¹²⁸

V. BRIEF OVERVIEW OF LITERATURE RESULTS FOR MOLECULES

The results that have been presented and discussed so far concern exclusively solid-state properties and may certainly

not reflect the trends for finite systems, as mentioned in Sec. III. Thus, in order to provide to the reader of the present work a more general view on the accuracy and applicability of the functionals, a very brief summary of some of the literature results for molecular systems is given below. To this end, we consider the atomization energy of strongly bound molecules and the interaction energy between weakly bound molecules, for which widely used standard testing sets exist.

A. Atomization energy of molecules

The atomization energy of molecules is one of the most used quantities to assess the performance of functionals for finite systems (see, e.g., Refs. 46, 48, 58, 69, 118, and 151 for recent tests). Large testing sets of small molecules like G3¹⁵² or W4-11¹⁵³ usually involve only elements of the first three periods of the periodic table. For such sets, the MAE given by LDA is typically in the range 70-100 kcal/mol (atomization energies are usually expressed in these units), while the best GGAs (e.g., BLYP) can achieve a MAE in the range 5-10 kcal/mol. MGGAs and hybrid can reduce further the MAE below 5 kcal/mol. At the moment, the most accurate functionals lead to MAE in the range 2.5-3.5 kcal/mol, e.g., mBEEF⁴⁹ (see also Refs. 58 and 118), which is not far from the so-called *chemical accuracy* of 1 kcal/mol. Concerning the best functionals for the solid-state test sets that we have identified just above, the MGGAs MGGa_MS2 and SCAN, as well as the hybrid-MGGAs MGGa_MS2h and revTPSSH are also excellent for the atomization energy of molecule since they lead to rather small MAE around 5 kcal/mol.^{46,48,103} With the hybrid YSPBEsol0 (~HSEsol), which was the best functional for the lattice constant, the MAE is larger (around 10-15 kcal/mol⁴³). The weak GGAs WC and PBEsol improve only slightly over LDA since their MAE is as large as 40-60 kcal/mol,^{48,69} while the stronger GGA PBEint leads to a MAE around 20-30 kcal/mol.¹⁵⁴

Therefore, as mentioned in Sec. III, it really seems that the kinetic-energy density is a necessary ingredient in order to construct a functional that is among the best for both solid-state properties and the atomization energy of molecules, and some of the modern MGGAs like SCAN look promising in this respect. With GGAs, it looks like an unachievable task to get such universally good results. Hybrid-GGAs can improve upon the underlying GGA, however we have not been able to find an excellent functional in our test set. For instance, YSPBEsol (~HSEsol) is very good for solids, but not for molecules, while the reverse is true for PBE0 (small MAE of ~7 kcal/mol for molecules,¹⁰⁴ but average results for solids, see Table II).

B. S22 set of noncovalent complexes

The S22 set of molecular complexes,¹⁵⁸ which consists of 22 dimers of biological-relevance molecules bound by weak interactions (hydrogen-bonded, dispersion dominated, and mixed), has become a standard set for the testing of functionals since very accurate CCSD(T) interaction energies are available.¹⁵⁸⁻¹⁶⁰ A large number of functionals have already been assessed on the S22 set, and Table V summarizes the

TABLE V. Results from the literature (reference in last column) for the MAE (in kcal/mol) on the S22 testing set.

Functional	MAE	Reference
LDA		
LDA ⁸⁰	2.3	48
GGA		
PBEsol ⁸³	1.8	48
PBE ⁷³	2.8	48
RPBE ⁹²	5.2	49
revPBE ⁹¹	5.3	27
BLYP ^{93,94}	4.8, 8.8	106, 48
MGGA		
M06-L ¹⁵⁵	0.7	156
MVS ⁴⁷	0.8	47
SCAN ⁴⁸	0.9	48
mBEEF ⁴⁹	1.4	49
MGGa_MS0 ⁴⁵	1.8	49
MGGa_MS2 ⁴⁶	2.1	49
revTPSS ⁹⁵	3.4	49
TPSS ⁹⁶	3.7	48
hybrid-GGA		
HSE ¹³	2.4	156
PBE0 ^{99,100}	2.5	156
B3LYP ¹⁰²	3.8	27
hybrid-MGGA		
MVSh ⁴⁷	1.0	47
M06 ¹¹⁶	1.4	156
TPSS0 ^{96,98}	3.1	27
GGA+D		
BLYP-D3 ²⁷	0.2	106
BLYP-D3(BJ) ¹⁰⁶	0.2	106
PBE+TS ^{26,a}	0.3	156
PW86PBE-XDM(BR) ¹⁵⁷	0.3	157
revPBE-D3 ²⁷	0.4	106
revPBE-D3(BJ) ¹⁰⁶	0.4	106
PBE-D3 ²⁷	0.5	106
PBE-D3(BJ) ¹⁰⁶	0.5	106
MGGA+D		
TPSS-D3 ²⁷	0.3	106
TPSS-D3(BJ) ¹⁰⁶	0.3	106
MGGa_MS0-D3 ^{46,a}	0.3	46
MGGa_MS1-D3 ^{46,a}	0.3	46
MGGa_MS2-D3 ^{46,a}	0.3	46
hybrid-GGA+D		
B3LYP-D3(BJ) ¹⁰⁶	0.3	106
B3LYP-D3 ²⁷	0.4	106
PBE0-D3(BJ) ¹⁰⁶	0.5	106
PBE0-D3 ²⁷	0.6	106
hybrid-MGGA+D		
MGGa_MS2-D3 ^{46,a}	0.2	46
TPSS0-D3 ²⁷	0.4	106
TPSS0-D3(BJ) ¹⁰⁶	0.4	106
GGA+NL		
optB88-vdW ^{34,a}	0.2	34
C09x-vdW ¹³¹	0.3	131
VV10 ^{31,a}	0.3	31

TABLE V. (Continued.)

Functional	MAE	Reference
rev-vdW-DF2 ¹³²	0.5	132
vdW-DF ²⁸	1.5	34
MGGA+NL		
SCAN+rVV10 ¹²⁸	0.4	128
BEEF-vdW ⁶⁹	1.7	49

^aOne or several parameters were determined using the S22 set.

results taken from the literature for many of the functionals that we have considered in the present work. Also included are results for nonlocal van der Waals functionals (groups GGA+NL and MGGA+NL), two atom-pairwise dispersion methods [PBE+TS²⁶ and PW86PBE-XDM(BR)¹⁵⁷], and the highly parameterized Minnesota functionals M06 and M06-L¹¹⁶ (results for other highly parameterized functionals can be found in Refs. 118, 161, and 162). Since all these recent results are widely scattered in the literature, it is also timely to gather them in a single table (see also Ref. 35). As indicated in Table V, some of the functionals contain one or several parameters that were fitted using the CCSD(T) interaction energies of the S22 set.

From the results, it is rather clear that the dispersion-corrected functionals are more accurate. The MAE is usually in the range 0.2-0.5 kcal/mol, while it is above 1 kcal/mol for the methods without dispersion correction term, except M06-L, MVS, and SCAN (slightly below 1 kcal/mol). As already observed for the layered compounds in Sec. IV B 2, MVS is one of the best non-dispersion corrected functionals, which is probably due to the particular form of the enhancement factor that is a strongly decreasing function of s and α (see Fig. 2). The same can be said about SCAN, which is also one of the semilocal functionals which do not completely and systematically fail for weak interactions. The MAE obtained with MGGA_MS2 is rather large (2.1 kcal/mol), despite that it was the best MGGA for the rare-gas solids. Among the GGAs, PBEsol represents a good balance between LDA and PBE which overestimate and underestimate the interaction energies, respectively,⁴⁸ but leads to a MAE which is still rather high (1.8 kcal/mol). In the group of nonlocal vdW functionals, the early vdW-DF and recent BEEF-vdW are clearly less accurate (MAE around 1.5 kcal/mol) than the others like SCAN+rVV10. The largest MAE obtained with an atom-pairwise dispersion method is only 0.6 kcal/mol (PBE0-D3).

By considering all results for weak interactions discussed in this work (rare-gas solids, layered solids, and S22 molecules), the most important comments are the following. For the three sets of systems, the atom-pairwise methods show a clear improvement over the other methods. Such an improvement is (slightly) less visible with the nonlocal vdW functionals, especially for the rare-gas and layered solids, where only rev-vdW-DF2 seems to compete with the best atom-pairwise methods. In Ref. 128, the recent SCAN+rVV10 nonlocal functional has shown to be very good for layered solids and the molecules of the S22 test set, but no results for rare-gas solids are available

yet. Among the non-dispersion corrected functionals, only a few lead *occasionally* to more or less reasonable results. This concerns mainly the recent MGGA functionals MGGA_MS2, MVS, and SCAN; however, their accuracies are still clearly lower than the atom-pairwise methods.

VI. SUMMARY

A large number of exchange-correlation functionals have been tested for solid-state properties, namely, the lattice constant, bulk modulus, and cohesive energy. Functionals from the first four rungs of Jacob's ladder were considered (i.e., LDA, GGA, MGGA, and hybrid) and some of them were augmented with a D3/D3(BJ) term to account explicitly for the dispersion interactions. The testing set of solids was divided into two groups: the solids bound by strong interactions (i.e., covalent, ionic, or metallic) and those bound by weak interactions (e.g., dispersion). Furthermore, in order to give a broader view of the performance of some of the tested functionals, a section was devoted to a summary of the literature results on molecular systems for two properties: the atomization energy and intermolecular binding.

One of the purposes of this work was to assess the accuracy of some of the recently proposed functionals like the MGGAs MGGA_MS n , SCAN, and mBEEF, and to identify, eventually, a *universally good* functional. Another goal was to figure out how useful it is to mix HF exchange with semilocal exchange or to add a dispersion correction term. An attempt to provide a useful summary of the most important observations of this work is the following:

1. For the strongly bound solids (Table II), at least one functional of each rung of Jacob's ladder, except LDA, belongs to the group of the most accurate functionals. Although it is not always obvious to decide if a functional should be a member of this group or not, we can mention the GGAs WC, PBEsol, PBEalpha, PBEint, and SG4, the MGGAs MGGA_MS2 and SCAN, the hybrids YSPBEsol0, MGGA_MS2h, and revTPSSh, and the dispersion corrected methods PBE-D3/D3(BJ).
2. Thus, from point 1 it does not seem to be really necessary to go beyond the GGA approximation for strongly bound solids since a few of them are overall as accurate as the more sophisticated/expensive MGGA and hybrid functionals. However, the use of a MGGA or hybrid functional may be necessary for several reasons as explained in points 3 and 4 below.
3. As well known (see Sec. V A), no GGA can be excellent for both solids and molecules at the same time. MGGAs like MGGA_MS2 or SCAN are better in this respect. Thus, the use of a MGGA should be more recommended for systems involving both finite and infinite systems as exemplified in, e.g., Ref. 163.
4. If a qualitatively more accurate prediction of the band gap of semiconductors and insulators is also required, then a hybrid functional should be used since GGA band gaps are usually by far too small compared to experiment.⁴²⁻⁴⁴ Note, however, that hybrid functionals are not recommended for

- metallic systems.^{75,122,123} MGGAs do not really improve over GGAs for the band gap (see Refs. 164–166).
- The use of a dispersion correction for strongly bound solids is recommended for functionals which clearly overestimate the lattice constant (usually more pronounced for solids containing alkali atoms). However, it is only in the case of PBE-D3/D3(BJ) that the overall accuracy is really good. We also observed that many of the DFT-D3/D3(BJ) methods lead to large errors for the bulk modulus, despite small errors for the lattice constant.
 - Among the functionals that were not tested in the present work, SCAN+rVV10 should be of similar accuracy as SCAN for strongly bound solids, but significantly improves the results for weak interactions according to Ref. 128.
 - For the weakly bound systems, namely, the rare-gas solids (Table III), layered solids (Table IV), and intermolecular complexes (Table V), it was observed that none of the non-dispersion corrected functionals is able to give qualitatively correct results in most cases. This is expected since the physics of dispersion is not included in the construction of these functionals. At best, good results can occasionally be expected with some of the MGGAs (MGGA_MS2, MVS, SCAN, or M06-L).
 - For weak interactions, many of the DFT-D3/D3(BJ) methods (and some of the nonlocal ones) are much more reliable. The results from the literature obtained with the recent SCAN+rVV10¹²⁸ or B97M-V¹¹⁸ are promising, but since these functionals were proposed very recently, more tests are needed in order to have a more complete view of their general performance.

Finally, from the present and previously published works, a very short conclusion would be the following. At the present time, it seems that the only functionals, which can be among the most accurate for the geometry and energetics in *both* finite and infinite systems and for *both* strong and weak bondings, are MGGAs augmented with a dispersion term. These are not bad news, since MGGAs functionals are barely more expensive than GGAs and the addition of a pairwise or nonlocal dispersion term does not significantly increase the computational time. However, in order to avoid problems of transferability, a MGA should preferably be constructed with a relatively smooth enhancement factor. If qualitatively accurate band gaps are also needed, then such functionals should be mixed with HF exchange, but with the disadvantage of a significantly increased computational cost, especially for large molecules or periodic solids.

ACKNOWLEDGMENTS

This work was supported by the Project No. SFB-F41 (ViCoM) of the Austrian Science Fund.

¹A. D. Becke, *J. Chem. Phys.* **84**, 4524 (1986).

²J. P. Perdew and Y. Wang, *Phys. Rev. B* **33**, 8800 (1986).

³P. Hohenberg and W. Kohn, *Phys. Rev.* **136**, B864 (1964).

⁴W. Kohn and L. J. Sham, *Phys. Rev.* **140**, A1133 (1965).

⁵A. J. Cohen, P. Mori-Sánchez, and W. Yang, *Chem. Rev.* **112**, 289 (2012).

⁶K. Burke, *J. Chem. Phys.* **136**, 150901 (2012).

⁷A. D. Becke, *J. Chem. Phys.* **140**, 18A301 (2014).

⁸R. O. Jones, *Rev. Mod. Phys.* **87**, 897 (2015).

⁹J. P. Perdew and K. Schmidt, *AIP Conf. Proc.* **577**, 1 (2001).

¹⁰J. P. Perdew, A. Ruzsinszky, J. Tao, V. N. Staroverov, G. E. Scuseria, and G. I. Csonka, *J. Chem. Phys.* **123**, 062201 (2005).

¹¹A. D. Becke, *J. Chem. Phys.* **98**, 5648 (1993).

¹²D. M. Bylander and L. Kleinman, *Phys. Rev. B* **41**, 7868 (1990).

¹³J. Heyd, G. E. Scuseria, and M. Ernzerhof, *J. Chem. Phys.* **118**, 8207 (2003); **124**, 219906 (2006).

¹⁴J. Harl and G. Kresse, *Phys. Rev. B* **77**, 045136 (2008).

¹⁵T. Olsen and K. S. Thygesen, *Phys. Rev. B* **87**, 075111 (2013).

¹⁶J. Klimeš and A. Michaelides, *J. Chem. Phys.* **137**, 120901 (2012).

¹⁷Y. Zhao and D. G. Truhlar, *J. Chem. Theory Comput.* **1**, 415 (2005).

¹⁸J. Sun, B. Xiao, Y. Fang, R. Haunschild, P. Hao, A. Ruzsinszky, G. I. Csonka, G. E. Scuseria, and J. P. Perdew, *Phys. Rev. Lett.* **111**, 106401 (2013).

¹⁹X. Wu, M. C. Vargas, S. Nayak, V. Lotrich, and G. Scoles, *J. Chem. Phys.* **115**, 8748 (2001).

²⁰Q. Wu and W. Yang, *J. Chem. Phys.* **116**, 515 (2002).

²¹M. Hasegawa and K. Nishidate, *Phys. Rev. B* **70**, 205431 (2004).

²²S. Grimme, *J. Comput. Chem.* **25**, 1463 (2004).

²³S. Grimme, *J. Comput. Chem.* **27**, 1787 (2006).

²⁴F. Ortman, F. Bechstedt, and W. G. Schmidt, *Phys. Rev. B* **73**, 205101 (2006).

²⁵A. D. Becke and E. R. Johnson, *J. Chem. Phys.* **122**, 154104 (2005).

²⁶A. Tkatchenko and M. Scheffler, *Phys. Rev. Lett.* **102**, 073005 (2009).

²⁷S. Grimme, J. Antony, S. Ehrlich, and H. Krieg, *J. Chem. Phys.* **132**, 154104 (2010).

²⁸M. Dion, H. Rydberg, E. Schröder, D. C. Langreth, and B. I. Lundqvist, *Phys. Rev. Lett.* **92**, 246401 (2004); **95**, 109902(E) (2005).

²⁹K. Lee, E. D. Murray, L. Kong, B. I. Lundqvist, and D. C. Langreth, *Phys. Rev. B* **82**, 081101(R) (2010).

³⁰O. A. Vydrov and T. Van Voorhis, *Phys. Rev. Lett.* **103**, 063004 (2009).

³¹O. A. Vydrov and T. Van Voorhis, *J. Chem. Phys.* **133**, 244103 (2010).

³²R. Sabatini, T. Gorni, and S. de Gironcoli, *Phys. Rev. B* **87**, 041108(R) (2013).

³³K. Berland and P. Hyldgaard, *Phys. Rev. B* **89**, 035412 (2014).

³⁴J. Klimeš, D. R. Bowler, and A. Michaelides, *J. Phys.: Condens. Matter* **22**, 022201 (2010).

³⁵S. Grimme, *Wiley Interdiscip. Rev.: Comput. Mol. Sci.* **1**, 211 (2011).

³⁶K. Berland, V. R. Cooper, K. Lee, E. Schröder, T. Thonhauser, P. Hyldgaard, and B. I. Lundqvist, *Rep. Prog. Phys.* **78**, 066501 (2015).

³⁷J. Harl, L. Schimka, and G. Kresse, *Phys. Rev. B* **81**, 115126 (2010).

³⁸L. Schimka, R. Gaudoin, J. Klimeš, M. Marsman, and G. Kresse, *Phys. Rev. B* **87**, 214102 (2013).

³⁹J. Yan and J. K. Nørskov, *Phys. Rev. B* **88**, 245204 (2013).

⁴⁰L. Shulenburger and T. R. Mattsson, *Phys. Rev. B* **88**, 245117 (2013).

⁴¹G. H. Booth, A. Grüneis, G. Kresse, and A. Alavi, *Nature* **493**, 365 (2013).

⁴²J. Heyd, J. E. Peralta, G. E. Scuseria, and R. L. Martin, *J. Chem. Phys.* **123**, 174101 (2005).

⁴³L. Schimka, J. Harl, and G. Kresse, *J. Chem. Phys.* **134**, 024116 (2011).

⁴⁴P. Pernet, B. Civalieri, D. Presti, and A. Savin, *J. Phys. Chem. A* **119**, 5288 (2015).

⁴⁵J. Sun, B. Xiao, and A. Ruzsinszky, *J. Chem. Phys.* **137**, 051101 (2012).

⁴⁶J. Sun, R. Haunschild, B. Xiao, I. W. Bulik, G. E. Scuseria, and J. P. Perdew, *J. Chem. Phys.* **138**, 044113 (2013).

⁴⁷J. Sun, J. P. Perdew, and A. Ruzsinszky, *Proc. Natl. Acad. Sci. U. S. A.* **112**, 685 (2015).

⁴⁸J. Sun, A. Ruzsinszky, and J. P. Perdew, *Phys. Rev. Lett.* **115**, 036402 (2015).

⁴⁹J. Wellendorff, K. T. Lundgaard, K. W. Jacobsen, and T. Bligaard, *J. Chem. Phys.* **140**, 144107 (2014).

⁵⁰F. Tran, R. Laskowski, P. Blaha, and K. Schwarz, *Phys. Rev. B* **75**, 115131 (2007).

⁵¹M. Ropo, K. Kokko, and L. Vitos, *Phys. Rev. B* **77**, 195445 (2008).

⁵²A. E. Mattsson, R. Armiento, J. Paier, G. Kresse, J. M. Wills, and T. R. Mattsson, *J. Chem. Phys.* **128**, 084714 (2008).

⁵³G. I. Csonka, J. P. Perdew, A. Ruzsinszky, P. H. T. Philipsen, S. Lebègue, J. Paier, O. A. Vydrov, and J. G. Ángyán, *Phys. Rev. B* **79**, 155107 (2009).

⁵⁴P. Haas, F. Tran, and P. Blaha, *Phys. Rev. B* **79**, 085104 (2009); **79**, 209902(E) (2009).

⁵⁵P. Haas, F. Tran, P. Blaha, L. S. Pedroza, A. J. R. da Silva, M. M. Odashima, and K. Capelle, *Phys. Rev. B* **81**, 125136 (2010).

⁵⁶J. Sun, M. Marsman, G. I. Csonka, A. Ruzsinszky, P. Hao, Y.-S. Kim, G. Kresse, and J. P. Perdew, *Phys. Rev. B* **84**, 035117 (2011).

⁵⁷P. Hao, Y. Fang, J. Sun, G. I. Csonka, P. H. T. Philipsen, and J. P. Perdew, *Phys. Rev. B* **85**, 014111 (2012); **85**, 099903 (2012).

⁵⁸R. Peverati and D. G. Truhlar, *Phys. Chem. Chem. Phys.* **14**, 13171 (2012).

- ⁵⁹P. Janthon, S. M. Kozlov, F. Viñes, J. Limtrakul, and F. Illas, *J. Chem. Theory Comput.* **9**, 1631 (2013).
- ⁶⁰L. A. Constantin, A. Terentjev, F. Della Sala, P. Cortona, and E. Fabiano, *Phys. Rev. B* **93**, 045126 (2016).
- ⁶¹M. J. Lucero, T. M. Henderson, and G. E. Scuseria, *J. Phys.: Condens. Matter* **24**, 145504 (2012).
- ⁶²R. Peverati and D. G. Truhlar, *Phys. Chem. Chem. Phys.* **14**, 16187 (2012).
- ⁶³P. Janthon, S. Luo, S. M. Kozlov, F. Viñes, J. Limtrakul, D. G. Truhlar, and F. Illas, *J. Chem. Theory Comput.* **10**, 3832 (2014).
- ⁶⁴M. Räsander and M. A. Moram, *J. Chem. Phys.* **143**, 144104 (2015).
- ⁶⁵J. Klimeš, D. R. Bowler, and A. Michaelides, *Phys. Rev. B* **83**, 195131 (2011).
- ⁶⁶T. Björkman, A. Gulans, A. V. Krashennnikov, and R. M. Nieminen, *J. Phys.: Condens. Matter* **24**, 424218 (2012).
- ⁶⁷T. Björkman, *Phys. Rev. B* **86**, 165109 (2012).
- ⁶⁸T. Björkman, *J. Chem. Phys.* **141**, 074708 (2014).
- ⁶⁹J. Wellendorff, K. T. Lundgaard, A. Møgelhøj, V. Petzold, D. D. Landis, J. K. Nørskov, T. Bligaard, and K. W. Jacobsen, *Phys. Rev. B* **85**, 235149 (2012).
- ⁷⁰J. Park, B. D. Yu, and S. Hong, *Curr. Appl. Phys.* **15**, 885 (2015).
- ⁷¹P. Blaha, K. Schwarz, G. K. H. Madsen, D. Kvasnicka, and J. Luitz, *WIEN2K: An Augmented Plane Wave Plus Local Orbitals Program for Calculating Crystal Properties* (Vienna University of Technology, Austria, 2001).
- ⁷²D. J. Singh and L. Nordström, *Planewaves, Pseudopotentials and the LAPW Method*, 2nd ed. (Springer, Berlin, 2006).
- ⁷³J. P. Perdew, K. Burke, and M. Ernzerhof, *Phys. Rev. Lett.* **77**, 3865 (1996); **78**, 1396(E) (1997).
- ⁷⁴F. Tran and P. Blaha, *Phys. Rev. B* **83**, 235118 (2011).
- ⁷⁵F. Tran, D. Koller, and P. Blaha, *Phys. Rev. B* **86**, 134406 (2012).
- ⁷⁶K. Lejaeghere, V. Van Speybroeck, G. Van Oost, and S. Cottenier, *Crit. Rev. Solid State Mater. Sci.* **39**, 1 (2014).
- ⁷⁷K. Rościszewski, B. Paulus, P. Fulde, and H. Stoll, *Phys. Rev. B* **62**, 5482 (2000).
- ⁷⁸S. Lebègue, J. Harl, T. Gould, J. G. Ángyán, G. Kresse, and J. F. Dobson, *Phys. Rev. Lett.* **105**, 196401 (2010).
- ⁷⁹T. Björkman, A. Gulans, A. V. Krashennnikov, and R. M. Nieminen, *Phys. Rev. Lett.* **108**, 235502 (2012).
- ⁸⁰J. P. Perdew and Y. Wang, *Phys. Rev. B* **45**, 13244 (1992).
- ⁸¹Z. Wu and R. E. Cohen, *Phys. Rev. B* **73**, 235116 (2006); Y. Zhao and D. G. Truhlar, *ibid.* **78**, 197101 (2008); Z. Wu and R. E. Cohen, *ibid.* **78**, 197102 (2008).
- ⁸²Y. Zhao and D. G. Truhlar, *J. Chem. Phys.* **128**, 184109 (2008).
- ⁸³J. P. Perdew, A. Ruzsinszky, G. I. Csonka, O. A. Vydrov, G. E. Scuseria, L. A. Constantin, X. Zhou, and K. Burke, *Phys. Rev. Lett.* **100**, 136406 (2008); **102**, 039902(E) (2008); A. E. Mattsson, R. Armiento, and T. R. Mattsson, *ibid.* **101**, 239701 (2008); J. P. Perdew, A. Ruzsinszky, G. I. Csonka, O. A. Vydrov, G. E. Scuseria, L. A. Constantin, X. Zhou, and K. Burke, *ibid.* **101**, 239702 (2008).
- ⁸⁴R. Armiento and A. E. Mattsson, *Phys. Rev. B* **72**, 085108 (2005).
- ⁸⁵E. Fabiano, L. A. Constantin, and F. Della Sala, *Phys. Rev. B* **82**, 113104 (2010).
- ⁸⁶G. K. H. Madsen, *Phys. Rev. B* **75**, 195108 (2007).
- ⁸⁷A. Ruzsinszky, G. I. Csonka, and G. E. Scuseria, *J. Chem. Theory Comput.* **5**, 763 (2009).
- ⁸⁸J. P. Perdew, J. A. Chevary, S. H. Vosko, K. A. Jackson, M. R. Pederson, D. J. Singh, and C. Fiolhais, *Phys. Rev. B* **46**, 6671 (1992); **48**, 4978(E) (1993).
- ⁸⁹P. Haas, F. Tran, P. Blaha, and K. Schwarz, *Phys. Rev. B* **83**, 205117 (2011).
- ⁹⁰R. Sarmiento-Pérez, S. Botti, and M. A. L. Marques, *J. Chem. Theory Comput.* **11**, 3844 (2015).
- ⁹¹Y. Zhang and W. Yang, *Phys. Rev. Lett.* **80**, 890 (1998).
- ⁹²B. Hammer, L. B. Hansen, and J. K. Nørskov, *Phys. Rev. B* **59**, 7413 (1999).
- ⁹³A. D. Becke, *Phys. Rev. A* **38**, 3098 (1988).
- ⁹⁴C. Lee, W. Yang, and R. G. Parr, *Phys. Rev. B* **37**, 785 (1988).
- ⁹⁵J. P. Perdew, A. Ruzsinszky, G. I. Csonka, L. A. Constantin, and J. Sun, *Phys. Rev. Lett.* **103**, 026403 (2009); **106**, 179902 (2011).
- ⁹⁶J. Tao, J. P. Perdew, V. N. Staroverov, and G. E. Scuseria, *Phys. Rev. Lett.* **91**, 146401 (2003).
- ⁹⁷J. P. Perdew, S. Kurth, A. Zupan, and P. Blaha, *Phys. Rev. Lett.* **82**, 2544 (1999); **82**, 5179(E) (1999).
- ⁹⁸J. P. Perdew, M. Ernzerhof, and K. Burke, *J. Chem. Phys.* **105**, 9982 (1996).
- ⁹⁹M. Ernzerhof and G. E. Scuseria, *J. Chem. Phys.* **110**, 5029 (1999).
- ¹⁰⁰C. Adamo and V. Barone, *J. Chem. Phys.* **110**, 6158 (1999).
- ¹⁰¹A. V. Krukau, O. A. Vydrov, A. F. Izmaylov, and G. E. Scuseria, *J. Chem. Phys.* **125**, 224106 (2006).
- ¹⁰²P. A. Stephens, F. J. Devlin, C. F. Chabalowski, and M. J. Frisch, *J. Phys. Chem.* **98**, 11623 (1994).
- ¹⁰³G. I. Csonka, J. P. Perdew, and A. Ruzsinszky, *J. Chem. Theory Comput.* **6**, 3688 (2010).
- ¹⁰⁴V. N. Staroverov, G. E. Scuseria, J. Tao, and J. P. Perdew, *J. Chem. Phys.* **119**, 12129 (2003); **121**, 11507 (2004).
- ¹⁰⁵L. Goerigk and S. Grimme, *Phys. Chem. Chem. Phys.* **13**, 6670 (2011).
- ¹⁰⁶S. Grimme, S. Ehrlich, and L. Goerigk, *J. Comput. Chem.* **32**, 1456 (2011).
- ¹⁰⁷See <http://www.thch.uni-bonn.de/tc/dftd3> for homepage of the D3-correction.
- ¹⁰⁸J. Moellmann and S. Grimme, *J. Phys. Chem. C* **118**, 7615 (2014).
- ¹⁰⁹A. Hoffmann, M. Rohrmüller, A. Jesser, I. dos Santos Vieira, W. G. Schmidt, and S. Herres-Pawlis, *J. Comput. Chem.* **35**, 2146 (2014).
- ¹¹⁰P. A. M. Dirac, *Proc. Cambridge Philos. Soc.* **26**, 376 (1930).
- ¹¹¹R. Gáspár, *Acta Phys. Hung.* **3**, 263 (1954).
- ¹¹²C. F. v. Weizsäcker, *Z. Phys.* **96**, 431 (1935).
- ¹¹³L. H. Thomas, *Proc. Cambridge Philos. Soc.* **23**, 542 (1927).
- ¹¹⁴E. Fermi, *Rend. Accad. Naz. Lincei* **6**, 602 (1927).
- ¹¹⁵P. Haas, F. Tran, P. Blaha, K. Schwarz, and R. Laskowski, *Phys. Rev. B* **80**, 195109 (2009).
- ¹¹⁶Y. Zhao and D. G. Truhlar, *Theor. Chem. Acc.* **120**, 215 (2008).
- ¹¹⁷E. R. Johnson, A. D. Becke, C. D. Sherrill, and G. A. DiLabio, *J. Chem. Phys.* **131**, 034111 (2009).
- ¹¹⁸N. Mardirossian and M. Head-Gordon, *J. Chem. Phys.* **142**, 074111 (2015).
- ¹¹⁹G. K. H. Madsen, L. Ferrighi, and B. Hammer, *J. Phys. Chem. Lett.* **1**, 515 (2010).
- ¹²⁰H. Iikura, T. Tsuneda, T. Yanai, and K. Hirao, *J. Chem. Phys.* **115**, 3540 (2001).
- ¹²¹T. Shimazaki and Y. Asai, *Chem. Phys. Lett.* **466**, 91 (2008).
- ¹²²Y.-R. Jang and B. D. Yu, *J. Phys. Soc. Jpn.* **81**, 114715 (2012).
- ¹²³W. Gao, T. A. Abtew, T. Cai, Y.-Y. Sun, S. Zhang, and P. Zhang, *Solid State Commun.* **234-235**, 10 (2016).
- ¹²⁴E. R. Johnson and A. D. Becke, *J. Chem. Phys.* **124**, 174104 (2006).
- ¹²⁵A. Koide, *J. Phys. B: At. Mol. Phys.* **9**, 3173 (1976).
- ¹²⁶See supplementary material at <http://dx.doi.org/10.1063/1.4948636> for the detailed results for the strongly bound solids and the DFT-D3/D3(BJ) results without three-body term for the layered solids.
- ¹²⁷J. Moellmann, S. Ehrlich, R. Tonner, and S. Grimme, *J. Phys.: Condens. Matter* **24**, 424206 (2012).
- ¹²⁸H. Peng, Z.-H. Yang, J. Sun, and J. P. Perdew, e-print [arXiv:1510.05712](https://arxiv.org/abs/1510.05712).
- ¹²⁹J. Tao, J. P. Perdew, and A. Ruzsinszky, *Phys. Rev. B* **81**, 233102 (2010).
- ¹³⁰F. Tran and J. Hutter, *J. Chem. Phys.* **138**, 204103 (2013); **139**, 039903 (2013).
- ¹³¹V. R. Cooper, *Phys. Rev. B* **81**, 161104(R) (2010).
- ¹³²I. Hamada, *Phys. Rev. B* **89**, 121103(R) (2014).
- ¹³³M. Callens and I. Hamada, *Phys. Rev. B* **91**, 195103 (2015).
- ¹³⁴W. A. Al-Saidi, V. K. Voora, and K. D. Jordan, *J. Chem. Theory Comput.* **8**, 1503 (2012).
- ¹³⁵T. Bučko, S. Lebègue, J. Hafner, and J. G. Ángyán, *Phys. Rev. B* **87**, 064110 (2013).
- ¹³⁶A. Tkatchenko, R. A. DiStasio, Jr., R. Car, and M. Scheffler, *Phys. Rev. Lett.* **108**, 236402 (2012).
- ¹³⁷O. Kullie and T. Saue, *Chem. Phys.* **395**, 54 (2012).
- ¹³⁸D. Roy, M. Marianski, N. T. Maitra, and J. J. Dannenberg, *J. Chem. Phys.* **137**, 134109 (2012).
- ¹³⁹A. Patra, B. Xiao, and J. P. Perdew, *Top. Curr. Chem.* **365**, 53 (2015).
- ¹⁴⁰G. Graziano, J. Klimeš, F. Fernandez-Alonso, and A. Michaelides, *J. Phys.: Condens. Matter* **24**, 424216 (2012).
- ¹⁴¹C. R. C. Rêgo, L. N. Oliveira, P. Tereshchuk, and J. L. F. Da Silva, *J. Phys.: Condens. Matter* **27**, 415502 (2015); **28**, 129501 (2016).
- ¹⁴²S. Kristyán and P. Pulay, *Chem. Phys. Lett.* **229**, 175 (1994).
- ¹⁴³J. M. Pérez-Jordá and A. D. Becke, *Chem. Phys. Lett.* **233**, 134 (1995).
- ¹⁴⁴X. Xu, Q. Zhang, R. P. Muller, and W. A. Goddard III, *J. Chem. Phys.* **122**, 014105 (2005).
- ¹⁴⁵A. Tkatchenko and O. A. von Lilienfeld, *Phys. Rev. B* **78**, 045116 (2008).
- ¹⁴⁶E. H. Lieb and S. Oxford, *Int. J. Quantum Chem.* **19**, 427 (1981).
- ¹⁴⁷T. A. Wesolowski, O. Parisel, Y. Ellinger, and J. Weber, *J. Phys. Chem. A* **101**, 7818 (1997).
- ¹⁴⁸Y. Zhang, W. Pan, and W. Yang, *J. Chem. Phys.* **107**, 7921 (1997).
- ¹⁴⁹Y. Zhao and D. G. Truhlar, *J. Phys. Chem. A* **110**, 5121 (2006).
- ¹⁵⁰L. Spanu, S. Sorella, and G. Galli, *Phys. Rev. Lett.* **103**, 196401 (2009).

- ¹⁵¹E. Fabiano, L. A. Constantin, A. Terentjevs, F. Della Sala, and P. Cortona, *Theor. Chem. Acc.* **134**, 139 (2015).
- ¹⁵²L. A. Curtiss, K. Raghavachari, P. C. Redfern, and J. A. Pople, *J. Chem. Phys.* **112**, 7374 (2000).
- ¹⁵³A. Karton, S. Daon, and J. M. L. Martin, *Chem. Phys. Lett.* **510**, 165 (2011).
- ¹⁵⁴E. Fabiano, L. A. Constantin, and F. Della Sala, *Int. J. Quantum Chem.* **113**, 673 (2013).
- ¹⁵⁵Y. Zhao and D. G. Truhlar, *J. Chem. Phys.* **125**, 194101 (2006).
- ¹⁵⁶N. Marom, A. Tkatchenko, M. Rossi, V. V. Gobre, O. Hod, M. Scheffler, and L. Kronik, *J. Chem. Theory Comput.* **7**, 3944 (2011).
- ¹⁵⁷F. O. Kannemann and A. D. Becke, *J. Chem. Theory Comput.* **6**, 1081 (2010).
- ¹⁵⁸P. Jurečka, J. Šponer, J. Černý, and P. Hobza, *Phys. Chem. Chem. Phys.* **8**, 1985 (2006).
- ¹⁵⁹T. Takatani, E. G. Hohenstein, M. Malagoli, M. S. Marshall, and C. D. Sherrill, *J. Chem. Phys.* **132**, 144104 (2010).
- ¹⁶⁰R. Podeszwa, K. Patkowski, and K. Szalewicz, *Phys. Chem. Chem. Phys.* **12**, 5974 (2010).
- ¹⁶¹N. Mardirossian and M. Head-Gordon, *Phys. Chem. Chem. Phys.* **16**, 9904 (2014).
- ¹⁶²N. Mardirossian and M. Head-Gordon, *J. Chem. Phys.* **140**, 18A527 (2014).
- ¹⁶³J. Sun, M. Marsman, A. Ruzsinszky, G. Kresse, and J. P. Perdew, *Phys. Rev. B* **83**, 121410(R) (2011).
- ¹⁶⁴Y. Zhao and D. G. Truhlar, *J. Chem. Phys.* **130**, 074103 (2009).
- ¹⁶⁵B. Xiao, J. Sun, A. Ruzsinszky, J. Feng, R. Haunschild, G. E. Scuseria, and J. P. Perdew, *Phys. Rev. B* **88**, 184103 (2013).
- ¹⁶⁶Z.-h. Yang, H. Peng, J. Sun, and J. P. Perdew, *Phys. Rev. B* **93**, 205205 (2016).